HHS Public Access

Author manuscript

Sci Signal. Author manuscript; available in PMC 2019 June 11.

Published in final edited form as:

Sci Signal. ; 11(560): . doi:10.1126/scisignal.aat3178.

Crk adaptor proteins mediate actin-dependent T cell migration and mechanosensing induced by the integrin LFA-1

Nathan H. Roy[1,2], **Joanna L. MacKay**[3], **Tanner F. Robertson**[1,2], **Daniel A. Hammer**[3,4], and **Janis K. Burkhardt**[1,2,*]

[1]Department of Pathology and Laboratory Medicine, Children's Hospital of Philadelphia Research Institute, Philadelphia, PA, USA

[2]Perelman School of Medicine at the University of Pennsylvania, Philadelphia, PA, USA

[3]Department of Bioengineering, University of Pennsylvania, Philadelphia, PA, USA

[4]Department of Chemical and Biomolecular Engineering, University of Pennsylvania, Philadelphia, PA, USA.

Abstract

T cell entry into inflamed tissue involves firm adhesion, spreading, and migration of the T cells across endothelial barriers. These events depend on "outside-in" signals through which engaged integrins direct cytoskeletal reorganization. We investigated the molecular events that mediate this process and found that T cells from mice lacking expression of the adaptor protein Crk exhibited defects in phenotypes induced by the integrin lymphocyte function–associated antigen 1 (LFA-1); namely, actin polymerization, leading edge formation, and two-dimensional cell migration. Crk protein was an essential mediator of LFA-1 signaling–induced phosphorylation of the E3 ubiquitin ligase c-Cbl and its subsequent interaction with the phosphatidylinositol 3-kinase (PI3K) subunit p85, thus promoting PI3K activity and cytoskeletal remodeling. In addition, we found that Crk proteins was required for T cells to respond to changes in substrate stiffness, as measured by alterations in cell spreading and differential phosphorylation of the force-sensitive protein CasL. These findings identify Crk proteins as key intermediates coupling LFA-1 signals to actin remodeling and provide mechanistic insights into how T cells sense and respond to substrate stiffness.

Introduction

Cells interact with their environment by sensing a multitude of environmental cues and translating them into a coordinated biochemical response. In particular, integrin-ligand interactions are important for sensing and responding to neighboring cells and extracellular

*Corresponding author. jburkhar@pennmedicine.upenn.edu.

Author Contributions: NHR is responsible for the design and execution of all the experiments. JLM assisted with the shear flow data gathering and analysis. TFR optimized primary mouse $CD4^+$ T cell transductions for PIP_3 visualization. JKB and DAH oversaw the project and aided in data interpretation and conclusions. NHR and JKB wrote the manuscript.

Competing interest: The authors declare that they have no competing interests.

Data and materials availability: All data needed to evaluate the conclusions in the paper are present in the paper or the Supplementary Materials.

matrix (ECM) components, as well as providing points of traction for cell migration. Integrins play a particularly important role in the immune system, where they are essential for several processes, including trafficking of leukocytes to sites of inflammation (1). During an inflammatory response, integrins on the leukocyte surface are engaged by ligands expressed on the endothelial surface. This triggers a cascade of events starting with firm adhesion of the leukocyte to the vessel wall, migration of the leukocyte along the wall, and, ultimately, transendothelial migration (TEM) (2). Throughout this process the leukocyte responds to local inflammation-induced changes to the vascular endothelium, including upregulation of ligands for integrins and other adhesion receptors. During chronic inflammation, this is accompanied by vascular wall stiffening (3–5), a process that seems to further enhance TEM (6, 7). The integrin-dependent events that control leukocyte trafficking are finely tuned; recruitment of leukocytes to damaged or infected tissue is essential for immune defense, but uncontrolled immune cell infiltration can drive a pro-inflammatory cycle leading to chronic inflammatory disease. Thus, a mechanistic understanding of these events is essential for designing and implementing novel interventions.

One of the principal integrins responsible for lymphocyte trafficking is lymphocyte function-associated antigen 1 (LFA-1), which interacts with intercellular adhesion molecule (ICAM)-1/2/3 on the endothelial surface. *In vitro* studies of LFA-1/ICAM-1 interaction demonstrate that initial LFA-1 engagement is followed by an actin dependent adhesion strengthening process needed for firm adhesion to the vascular wall, as well as T cell polarization and crawling (8). Both firm adhesion and crawling on the vascular wall are important for efficient TEM (9–12). Notably, all these events depend directly on signals delivered by engaged integrins. In fact, effector T cells that are allowed to rest on ICAM-1 coated surfaces immediately undergo actin reorganization, polarize, and begin to migrate, demonstrating that ligation of LFA-1 alone is sufficient to stimulate the necessary signaling to drive T cell migration (13–15). It has become clear that many cell types can sense stiffness and other physical properties of their substrates and translate this information into a biochemical response (16, 17). This mechanosensing is likely to be important *in vivo,* where tissues are relatively soft compared to plastic or glass. Despite its importance, very little is known about the mechanisms underlying mechanosensing in T cells.

Most of the time, T cell integrins exist in a bent, inactive state, but signaling through chemokine receptors or the T cell receptor (TCR) triggers them to extend and become primed for ligand binding (18). This form of integrin regulation is called ‘inside-out’ signaling, and is governed by the interaction of the integrin cytoplasmic tails with proteins such as talin and kindlins, which cause large conformational changes along with receptor clustering, resulting in increased binding (19). Ligand binding then stabilizes the high affinity state and initiates an ‘outside-in’ signaling cascade that relays information about the environment to the cell’s interior. Although the molecular events that underlie inside-out signaling are relatively well defined [reviewed in (19, 20)], much less is known about outside-in signaling mechanisms, and most of what is known comes from study of neutrophils and other innate immune cells (21). In contrast, the outside-in signaling events that contribute to T cell migration are largely unexplored. One obstacle to progress in this area is the complex cascade: outside-in signals are necessarily preceded by inside-out signals, and several proteins seem to function in both pathways (19, 20, 22–28).

Among the proteins that function in the inside-out signaling pathway are the CT10 regulator of kinases (Crk) proteins, which we and others have shown link TCR and chemokine stimulation to Ras-related protein 1 (Rap-1) dependent integrin affinity modulation (29, 30). Crk proteins (CrkI, CrkII, and CrkL) are small adapter molecules with a modular Src homology 2 and Src homology 3 (SH2-SH3-SH3) domain structure. CrkII and the splice variant CrkI (lacking the C-terminal SH3 domain) are transcribed from the *Crk* locus, while CrkL is transcribed from a separate *CrkL* locus. Crk proteins are widely expressed and have many *in vivo* functions; knocking out either *Crk* or *CrkL* is lethal in mice (31, 32). In fibroblasts, Crk proteins localize to integrin based focal adhesions, and promote the stability of these structures (33–36). In keeping with this, Crk proteins have been implicated in adhesion related processes such as cell spreading and migration (37, 38) and Crk protein expression has been correlated with invasiveness of certain cancers (39, 40). Although there is limited information on Crk protein function in T cells, we recently showed that these proteins control T cell trafficking to sites of inflammation (30). T cells lacking Crk proteins showed defects in migration through an endothelial monolayer *in vitro*, and diminished tissue infiltration in a graft-versus-host disease model. Together, these findings point to a requirement for these proteins in one or more of the steps associated with TEM (30). While these defects could, in principle, be explained by the requirement for Crk proteins in inside-out signaling, we hypothesized that these proteins are also important for other aspects of T cell integrin function. Therefore in this study, we set out to analyze the role of Crk proteins downstream of engaged integrins, with the goal of uncovering previously unknown signaling events that mediate T cell spreading, migration, and mechanosensing.

Results

Crk proteins mediate adhesion strengthening

Using conditional knockout mice that delete both the *Crk* and *CrkL* loci in mature T cells (DKO mice), we previously showed that Crk proteins are required for TEM and trafficking into inflamed tissue (30). These defects are at least partially traceable to a requirement for Crk proteins in inside-out signaling events leading to integrin affinity modulation (29, 30). However, integrin engagement also leads to T cell spreading, cytoskeletal remodeling, and migration, all of which are important functions carried out by Crk proteins in non-hematopoietic cells (33–38). To test the role of Crk proteins in these cytoskeleton-dependent responses downstream of LFA-1, WT and DKO $CD4^+$ T cells were allowed to spread on ICAM-1 coated surfaces and F-actin was quantified at the cell-surface interface. As shown in Fig 1A-B, DKO T cells spread far less efficiently and had less F-actin staining than WT T cells. Two mechanistic defects could explain this phenotype: (i) activation of LFA-1 could be perturbed, leading to inefficient ICAM-1 binding, or (ii) signaling downstream of engaged LFA-1 could be disrupted. To differentiate between these two hypotheses, we examined whether the defect could be rescued by treating the cells with Mn^{2+}, which exogenously drives integrins into the active conformation, bypassing the need for inside-out signaling and affinity modulation (41). Alternatively, cells were stimulated with PMA, which directly activates actin regulatory pathways independent of integrin engagement. Treatment with PMA, but not Mn^{2+}, rescued the DKO phenotype (Fig. 1, A and B), showing that the defect lies in the signaling pathways downstream of LFA-1. Analysis of the effects

of increasing ICAM-1 dose shows that Mn^{2+} activated DKO T cells exhibit defective actin responses even at ICAM-1 abundance well beyond the saturation point for WT T cells (Fig. 1C), providing further evidence that the defects do not stem from diminished ligand binding. Notably, PMA-treated DKO T cells polymerized actin efficiently, indicating that DKO T cells can launch an actin response when outside-in integrins are bypassed. Because PMA is a potent PKC activator with broad effects, we also tested T cell responses downstream of a more physiological stimulus, TCR engagement. Both WT and DKO T cells spreading on surfaces coated with anti-CD3 (alone or together with ICAM-1) spread efficiently and generated the expected lamellipodial and lamellar actin-rich regions (Fig. 1D). Moreover, the amount of actin accumulation in WT and DKO T cells was indistinguishable. Taken together, these results show that Crk proteins are not required for actin polymerization *per se*, but rather for transmitting integrin signals to the actin regulatory machinery.

In light of these findings, we revisited our earlier study in which we found that DKO T cells exhibit diminished integrin-dependent adhesion (30). As previously reported, DKO T cells adhere poorly to ICAM-1, but this adhesion defect can be reversed by treatment of PMA or Mn^{2+} (Fig. 1E). Interestingly, Mn^{2+} treated DKO cells still adhered slightly less well than Mn^{2+} treated WT T cells, indicating that converting all integrins to the high affinity conformation is not sufficient to allow cells to resist the harsh wash steps used in this assay. Based on this observation, we hypothesized that Crk proteins are required for the integrin-dependent actin polymerization events that mediate cell spreading and adhesion strengthening. To assess adhesion under more physiological conditions, we turned to a flow chamber system that permits dissection of tethering and rolling, arrest, and firm adhesion/cell spreading. T cells were added to a flow chamber coated with ICAM-1, P-selectin, and stromal cell-derived factor 1 (SDF-1) to emulate inflamed endothelium, and then imaged under physiological shear conditions. WT and DKO T cells arrested equally well under shear flow, and this arrest was dependent on the LFA-1/ICAM-1 interaction (Fig. 1F). However, almost all the WT T cells assumed a spread (phase dark) morphology, whereas a significant percentage of adherent DKO T cells failed to spread (Fig. 1G). Moreover, when arrested T cells were subjected to stepwise increases in shear rate, DKO T cells detached more readily (Fig. 1H). Taken together, these data suggest that Crk proteins transmit signals from engaged LFA-1 to direct actin remodeling events leading to T cell spreading and adhesion strengthening.

Crk proteins regulate integrin-dependent T cell motility

In addition to mediating adhesion and cell spreading, the interaction of integrins with endothelial ligands stimulates cell motility, an important process during extravasation (8–12). To evaluate the role of Crk proteins in integrin-dependent motility, we imaged WT and DKO $CD4^+$ T cells migrating on ICAM-1 coated coverslips. Whereas the majority of WT T cells spread firmly on the surface and formed a broad leading edge, DKO T cells sat higher on the coverslip, and showed multiple pseudopodia. In keeping with their inability to form a single stable leading edge, these cells exhibited more frequent changes in direction (Fig 2A and movies S1 and S2). By imaging T cells expressing Lifeact-GFP, we confirmed that the leading edge in WT T cells was rich in actin, while DKO T cells failed to form this structure and instead seemed to extend multiple short-lived pseudopodia (Fig. 2B, movies S3 and S4).

Tracking studies showed that while 95% of both WT and DKO T cells were motile (Fig. 2C), DKO T cells exhibited lower average speed and diminished directionality (Fig. 2, D to F).

Depending on the environment through which they are moving, T cells can preferentially utilize two distinct modes of motility. In 2D settings where integrin ligands are abundant, T cells polymerize actin at the leading edge to drive keratocyte-like motility (or 'sliding'), whereas on low adhesive surfaces and in 3D settings where cells are confined, they default to myosin-based amoeboid motility (in low adhesive 2D settings, this has been described as 'walking') (42, 43). The morphology of migrating DKO T cells resembles that of T cells 'walking' on low adhesive surfaces. To test whether DKO T cells are particularly reliant on this myosin-dependent mode of motility, we treated WT and DKO T cells with the myosin ATPase inhibitor blebbistatin or the Rho-kinase inhibitor Y-27632, which inhibits myosin indirectly. In comparison to WT T cells, DKO T cells were highly sensitive to myosin inhibition; a higher percentage of DKO T cells became round and immobile upon treatment with either drug (Fig 3, A and B). We interpret this to mean that, unlike WT T cells, DKO T cells are unable to overcome myosin inhibition by switching to an actin based 'sliding' mechanism. In support of this view, we found that the subset of cells that remained mobile responded quite differently in terms of cell shape. When treated with myosin inhibitors, WT T cells switched to an exaggerated 'sliding' morphology with an extremely broad, flat leading edge (Fig. 3C). This change could be quantified as a reduction in the cellular length:width ratio (Fig. 3D). Before myosin inhibition, DKO T cells were more elongated than WT T cells, as evidenced by a higher length:width ratio. Upon treatment, DKO T cells showed a percent reduction in length:width ratio similar to that of WT cells. However, the shape of DKO T cells was quite distinct from that of WT cells. They remained more elongated than even untreated WT cells, and almost never formed a broad flat leading edge (Fig 3C). Thus, we conclude that Crk proteins facilitate the establishment of an actin rich cell front during integrin dependent migration, such that in the absence of Crk proteins, T cells default to myosin driven "walking" motility. These findings help to explain our earlier observation that Crk-deficient T cells migrate normally in 3D collagen gels but exhibit defects in transendothelial migration (30), since they can use myosin-dependent ameboid motility to move through the confined spaces in collagen gels, but use integrin-dependent motility to penetrate endothelial barriers.

Crk proteins are critical for Rho GTPase activation and recruitment of nucleation promoting factors at the leading edge.

To better understand how Crk proteins direct actin polymerization at the leading edge of migrating T cells, we next analyzed the distribution of Wiskott–Aldrich Syndrome protein (WASp) and WASP-family verprolin-homologous protein 2 (WAVE2), actin nucleation promoting factors that are activated by the Rho GTPases Cdc42 and Rac, respectively. T cells migrating on ICAM-1 were fixed and labeled with an antibody specific for the open, active form of WASp (44), or with an antibody that recognizes total WAVE2. In WT T cells, WAVE2 co-localized with actin at the leading edge. Open-WASp was also enriched in the leading edge, concentrating just behind the actin-rich region (Fig. 4, A and B). In contrast, DKO T cells showed no enrichment of either open-WASp or WAVE2 toward the front of the

cell (Fig. 4, A and B). To assess the activation of Cdc42 and Rac directly, GTPase pulldowns were performed. Rested $CD4^+$ T cell blasts from WT and DKO mice were left untreated or treated with Mn^{2+} to induce integrin activation. Cells were then stimulated with either soluble or surface-immobilized ICAM-1, lysed, and mixed with the PAK-PBD domain to capture GTP-bound Cdc42 and Rac1. WT T cells showed a significant increase in Cdc42 activity in response to surface bound, but not soluble, ICAM-1, while DKO T cells lacked this response (Fig. 4, C and D). Rac1 showed a similar activation pattern, though the results did not reach statistical significance due to variability in the WT T cell response.

Crk proteins promote integrin mediated phosphatidylinositol 3-kinase (PI3K) signaling

In an effort to understand where Crk proteins fit into the signaling pathway linking engaged LFA-1 to actin polymerization, we analyzed protein phosphorylation patterns in WT and DKO T cells treated with Mn^{2+} and stimulated with either soluble or surface-bound ICAM-1. Lysates were immunoblotted for total phospho-tyrosine (pTyr), as well as phospho-AKT and phospho-ERK. Robust protein phosphorylation took place only when cells were stimulated with surface-bound ICAM-1 (Fig. 5, A and B), consistent with the idea that outside-in LFA-1 signals involve an important mechanical component. The overall pattern of tyrosine phosphorylation was very similar in WT and DKO T cells, although we did observe a band of approximately 120kDa that was poorly phosphorylated in DKO T cells (Fig. 5A, arrow). ERK phosphorylation was unperturbed in DKO T cells. Interestingly, however, we found that phosphorylation of AKT was significantly diminished. Because AKT phosphorylation is a hallmark of phosphatidylinositol 3-kinase (PI3K) activity, this finding indicates that Crk proteins are needed for LFA-1 dependent PI3K activation. In support of this idea, Crk proteins have been implicated in PI3K signaling in fibroblasts and transformed cells (45–50).

To test the role of PI3K in cell spreading and actin polymerization downstream of LFA-1, Mn^{2+} treated WT and DKO T cells were allowed to spread on ICAM-1 in the presence of the pan PI3K inhibitor LY-294002 or two more specific inhibitors, IC87114 (PI3Kδ) and CZC24832 (PI3Kγ), and actin intensity was measured as described earlier (Fig. 1). All three PI3K inhibitors diminished the response of WT cells to amounts similar to DKO cells, while having no effect on DKO spreading and actin abundance (Fig. 5C). The product of PI3K, phosphatidylinositol (3,4,5)-trisphosphate (PIP_3), is an important molecule that influences cell shape, polarity, and migration (51). To monitor the localization of PIP_3, $CD4^+$ T cells were transduced with a GFP-tagged Pleckstrin homology (PH) domain of GRP1, which preferentially binds to PIP_3 (52), and imaged while migrating on ICAM-1 coated coverslips. Migrating WT T cells consistently displayed an accumulation of PIP_3 in the front third of the cell, while in DKO T cells PIP_3 was distributed over most of the plasma membrane, even when these cells showed a well polarized morphology (Fig. 5D). GFP signal was also evident in the nucleus of many cells, a compartment where this biosensor is known to accumulate, but even in such cells a change in the distribution of the cell surface pool could be observed. These results point toward a role for Crk proteins in LFA-1 dependent PI3K activation at the leading edge of migrating T cells.

Crk proteins promote Cbl phosphorylation and binding to the p85 subunit of PI3K

PI3K activity is controlled through the binding of the p85 regulatory subunit to phosphorylated tyrosines on interacting proteins. To ask if loss of Crk proteins affects the pattern of phosphorylated proteins associated with p85, WT and DKO T cells were stimulated with surface bound ICAM-1, and lysates were immunoprecipitated with anti-p85 and immunoblotted for pTyr. A pronounced band at 120kDa co-immunoprecipitated with p85 after stimulation with ICAM-1, and this interaction was dependent on Crk protein expression (Fig. 6A). Notably, a 120kDa tyrosine-phosphorylated protein also co-immunoprecipitated with CrkL after integrin engagement (Fig. 6B). Because this band resembles the 120kDa species found in an earlier experiment (Fig. 5), which was phosphorylated only when Crk proteins were present, it seemed likely that a single protein of 120kDa is tyrosine-phosphorylated in a Crk-dependent fashion and interacts with both CrkL and p85. To identify the relevant protein, CrkL immunoprecipitates were resolved on gels, and the region surrounding 120kDa was excised and subjected to mass spectrometry. Two interacting proteins were identified, Casitas B-lineage lymphoma protein (c-Cbl) and Casitas B-lineage lymphoma B (Cbl-b) (fig. S1). Parallel analysis of p85 immunoprecipitates yielded the same two species. To test the idea that Crk proteins regulate integrin-dependent phosphorylation of Cbl proteins, we stimulated WT and DKO cells with ICAM-1 as described above (Fig 5A), immunoprecipitated with anti-pTyr, and blotted for c-Cbl and Cbl-b. Engagement of surface bound ICAM-1 induced strong phosphorylation of both c-Cbl and Cbl-b in WT T cells, but this response was greatly diminished in DKO T cells (Fig. 6C). Of the two Cbl isoforms, phosphorylation of c-Cbl showed the greatest Crk dependency; c-Cbl phosphorylation was reduced ~90% while Cbl-b was reduced by only ~50%. Another phosphoprotein of ~120kDa that is important for integrin-dependent T cell migration (53, 54) is the kinase Pyk2. To rule out this alternate candidate, we monitored Pyk2 phosphorylation in WT and DKO T cells and found that Pyk2 phosphorylation does not depend on Crk protein expression (Fig. 6D). Together with the data on overall tyrosine phosphorylation patterns (Fig. 5A), these findings show that Crk proteins are not required for LFA-1 dependent tyrosine phosphorylation in general, but instead mediate very specific downstream pathways involving Cbl and PI3K.

Given the known adapter role of Crk proteins, it is likely that they promote cbl phosphorylation by bringing Cbl into proximity with tyrosine kinases. Since Crk proteins are known to coordinate the activity of both Src and Abl family kinases (37, 38), we asked if these kinase families were responsible for c-Cbl phosphorylation. Using PP2 to inhibit Src kinases and STI-571 to inhibit Abl kinases, we found that c-Cbl phosphorylation downstream of LFA-1 engagement was completely dependent on Src kinase activity (Fig. 6E), and independent of Abl family kinases. Taken together, our data support a model in which Crk proteins coordinate the Src dependent phosphorylation of c-Cbl downstream of integrin engagement, thereby creating a scaffold for p85 and ultimately leading to PI3K activity.

Crk proteins function in T cell mechanosensing

One of the most striking aspects of the LFA-1 dependent signaling events we have identified is the requirement for presentation of ICAM-1 as an immobilized ligand. Integrin

engagement *per se* is not sufficient to stimulate a robust response, suggesting a role for mechanotransduction. Indeed, since actin dynamics are important to generate force on bound ligands, we hypothesized that Crk proteins may tune mechanotransduction via effects on actin dynamics. To evaluate the response of T cells to the mechanical properties of the substrate, Mn^{2+} treated WT and DKO $CD4^{+}$ T cells were allowed to interact with ICAM-1 coated hydrogels of varying stiffness. Cells were then fixed, labeled with fluorescent phalloidin, and imaged as described in Figure 1. WT T cells responded to increasing substrate stiffness with increased actin polymerization and enhanced formation of a well-spread leading edge (Fig. 7A). This effect was most pronounced between 12 and 25 kPa. In contrast, DKO T cells lacked this response. Indeed, there was no significant change in actin polymerization in DKO T cells responding to surfaces of 4 vs 50kPa (Fig 7, A and B). This was not due to differences in ligand coating of the hydrogels, as all the stiffnesses bore comparable amounts of ICAM-1 (fig. S2).

In non-hematopoietic cells, Crk proteins are known to interact directly with the mechanosensing protein p130Cas, which undergoes force-dependent structural changes that render it primed for phosphorylation and downstream signaling (55). In T cells, the function of p130Cas is carried out by a hematopoietic homologue, CasL (also known as HEF1), which is constitutively associated with CrkL (fig. S3). While several recent papers implicate CasL in mechanotransduction at the immunological synapse (56–58), CasL function in integrin-dependent T cell responses has not been examined. We therefore measured CasL phosphorylation downstream of LFA-1 using the stimulation regime described earlier (Fig. 5A). CasL was phosphorylated upon integrin engagement, especially when integrin ligands were presented on a stimulatory surface, and this response was Crk dependent (Fig. 7C). We next evaluated CasL phosphorylation in T cells spreading on ICAM-1 coated hydrogels. Strikingly, we found in WT T cells that phosphorylation of CasL was strongly dependent on substrate stiffness, while this response was severely blunted in DKO T cells (Fig 7, D and E). These data indicate that Crk proteins function together with CasL to help T cells integrate mechanical cues from engaged integrins.

Mechanosensing depends on forces generated by the cytoskeleton, which induce conformational changes needed for events such as Cas protein phosphorylation and integrin activation. Given our findings that Crk proteins direct actin reorganization downstream of LFA-1, we investigated whether CasL phosphorylation involves the actin cytoskeleton. T cells interacting with ICAM-1 coated surfaces were treated with latrunculin B to depolymerize actin filaments or with blebbistatin to inhibit contraction of the acto-myosin network. Treatment with latrunculin B reduced pCasL to control amounts, whereas treatment with blebbistatin had no effect (Fig. 7F). Notably, phosphorylation of c-Cbl was unaffected by either treatment, showing that cytoskeletal forces are not important for this phosphorylation event. Thus, although both CasL and c-Cbl bind to Crk proteins and depend on Crk proteins for their phosphorylation, the molecular requirements for these events are distinct. To better understand this distinction, we compared the binding of CrkL to c-Cbl and CasL before and after integrin engagement. This analysis revealed that binding of CrkL to CasL is constitutive, whereas binding of CrkL to c-Cbl to is induced by integrin engagement (fig. S2). Thus, our data support a mechanosensory signaling model in which CrkL is pre-associated with CasL in resting cells. LFA-1 engagement induces CrkL binding to c-Cbl and

Src-dependent c-Cbl phosphorylation. This, in turn, leads to actin polymerization and generation of the forces needed for CasL phosphorylation (Fig. 8).

Discussion

We showed previously that T cells lacking Crk proteins exhibit defects in inside-out signaling events needed for Rap-1 dependent integrin activation and migration to sites of inflammation (30). Here, we show that Crk proteins also serve as key signaling intermediates linking integrin engagement to actin responses. Downstream of integrins, Crk proteins coordinate two interrelated sets of events, adhesion-dependent motility and substrate mechanosensing. Intriguingly, both of these processes are required for TEM. These studies shed new light on the molecular pathways through which integrins interpret environmental cues and coordinate cell migration through body tissues.

Engagement of LFA-1 stimulates complex cytoskeletal changes needed for directed cell movement (13–15), but the relevant signaling pathways are poorly defined. Early studies showed that although T cells lack obvious focal adhesions, integrin engagement induces phosphorylation of adhesion associated proteins including FAK, Pyk2, c-Cbl, and CasL (59, 60). Importantly, we now show that the majority of tyrosine phosphorylation events downstream of LFA-1 require immobilized ICAM-1, consistent with a force-dependent signaling mechanism. While Crk proteins are dispensable for most signaling events, they are critical for phosphorylation of c-Cbl and binding of c-Cbl to the p85 subunit of PI3K. Although c-Cbl is best known as an ubiquitin ligase (61–66), it probably functions primarily as a scaffolding molecule in this setting. Our results are consistent with findings in BCR-Abl transformed cells, where hyper-phosphorylation of c-Cbl results in it's binding to p85 and PI3K activation (67–70). Engagement of T cell integrins has previously been shown to activate PI3K (71–73); our studies identify Crk proteins and c-Cbl as novel intermediates in this pathway (Fig 8).

Exactly how Crk proteins promote phosphorylation of c-Cbl remains unknown, but our results point to the involvement of Src family kinases. In macrophages, integrin engagement leads to the Src dependent phosphorylation of c-Cbl and ultimately PI3K activity (74). It will be interesting to assess the role of Crk proteins in these cells to determine if this pathway is common among immune cells or unique to T cells. It will also be interesting to ask whether CrkII and CrkL play unique or redundant roles in the pathways defined here. Though these two Crk isoforms are closely related, they are regulated quite differently (75). Our previous studies on transendothelial migration point to at least some functional redundancy (30), however T cells lacking *CrkL* exhibit more profound defects in several assays of integrin function (30). We show here that CrkL binds to c-Cbl and CasL; it remains to be determined whether CrkII behaves similarly.

Disrupting the Crk signaling cascade had profound effects on actin dependent processes such as cell spreading and migration. These effects were specific to integrin signaling, since TCR-dependent actin responses were intact. The cytoskeletal defects we observe in Crk-deficient cells are associated with decreased activation of the Rho GTPases Cdc42 and Rac, and changes in the distribution of their effectors WASp and WAVE2. This may trace back to

decreased activation of PI3K, since PI3K generates inositol lipid docking sites for regulatory GEFs and GAPs (76). It remains possible, however, that Crk proteins affect Rho GTPase activation through a PI3K independent mechanism. Indeed, Crk proteins can directly bind to Rac GEFs such as DOCK180 in non-hematopoietic cells (77, 78) and DOCK2 in lymphoid cells (79). Future work aimed at identifying Crk binding proteins under resting and integrin-stimulated conditions should deepen the mechanistic understanding of LFA-1 signaling.

One major consequence of the altered actin responses in Crk deficient T cells was a change in the dominant mode of cell motility. Leukocyte motility is highly plastic (80, 81), and T cells exhibit different modes of motility depending on environmental cues (42, 43). Generally speaking, ‘walking’ (amoeboid motility) is the preferred mechanism of migration in 3D environments, while ‘sliding’ (keratocyte-like motility) occurs on highly adhesive 2D surfaces. We show that Crk proteins are particularly important for sliding motility, which relies heavily on actin polymerization at the leading edge. Interestingly, we previously documented that DKO T cells migrate normally in 3D collagen gels (30), indicating that Crk proteins are dispensable for amoeboid motility. Sliding motility may be particularly important during extravasation, where integrin interactions are essential for migration along the ligand-rich surface of the inflamed vascular wall, in search of favorable sites for transmigration.

Integrins directly link the extracellular environment to the internal cytoskeleton and thus can act as physical probes of the substrate (17, 82). We show that T cell integrins function as mechanosensors, triggering stiffness-dependent actin polymerization and CasL phosphorylation. The CasL response is especially intriguing, since Cas family proteins are thought to be important for mechanosensing in non-hematopoietic cells (55, 83–85), and CasL has been proposed to function as a T cell force sensor at the immunological synapse (56–58). Stiffness-dependent CasL phosphorylation and actin polymerization were severely blunted in DKO T cells, highlighting the role of Crk signaling in T cell mechanosensing. Phosphorylation of Cas family proteins is augmented by actin flow (58, 86), which is thought to provide the forces needed to expose stretch dependent phosphorylation sites. Consistent with this view, we find that inhibiting actin dynamics in WT T cells blocks CasL phosphorylation. Thus, we propose that Crk proteins function in mechanosensing indirectly, by stimulating local actin polymerization (Fig 8). Because Crk signaling only takes place when LFA-1 interacts with surface-bound ICAM-1, this system may provide a feedback mechanism that selectively sustains signaling when integrins are engaged to ligands capable of providing counter-force, an important factor during mechanosensing as well as cell migration.

As T cells crawl along the endothelium, small invadopodia-like protrusions originating from the T cell push into the underlying endothelium (87–89). These protrusions act as mechanical probes, interrogating the endothelial monolayer for areas that are relatively soft and amenable to diapedesis (89). Interestingly, formation of invadopodia-like protrusions is dependent upon activation of Cdc42 (88). Based on our findings that Crk proteins regulate both Cdc42 activation and mechanical signals downstream of LFA-1 engagement, we propose that Crk proteins mediate mechanochemical crosstalk between T cells and the vascular endothelium. If so, Crk proteins and their associated pathways could be important

therapeutic targets in chronic inflammatory conditions such as atherosclerosis, where increases in vascular stiffness contribute to disease progression (3, 4, 90).

An important area for future exploration is the role of Crk proteins at the immunological synapse, where engagement of the TCR together with LFA-1 induces adhesion, actin polymerization, and co-stimulation (24, 25, 91, 92). Biochemical analysis shows that TCR engagement results in the formation of signaling complexes containing Crk proteins, c-Cbl, and p85, although the functional relevance of this is still unclear (93–97). Notably, a recent study found that the spatial regulation of Crk at the synapse was crucial for its function in controlling Rap-1 activation and integrin-dependent adhesion (98). Finally, in light of our work, it will be important to investigate whether Crk proteins contribute to mechanosensing during T cell activation. T cells probe antigen presenting cells much as they do endothelia (99), and T cell activation is sensitive to the mechanical properties of stimulatory surfaces (100–103). Thus, it seems likely that Crk proteins will prove to function together with PI3K, CasL, WASp, and Cdc42 to direct mechanical signaling during T cell activation.

Materials and Methods

Antibodies and reagents

Anti-CD3 clone 2C-11, anti-CD28 clone PV1, and LFA-1 blocking anti-CD11a clone M17/4 were obtained from BioXCell. Anti-pTyr clone PY-20 and anti-p85 (ABS234) was from Upsate (Millipore). Anti-HEF1 (CasL) clone 2G9 and anti-Pyk2 clone YE353 were obtained from Abcam. Anti-Rac1 (610650) and anti-AKT (559028) were from BD. Anti-pAKT (4051), anti-pERK (9101), and anti-c-Cbl (2747) were from Cell Signaling. Anti-Cdc42 (SC-87), anti-CrkL (SC-319), and anti-Cbl-b (SC-8006) were from Santa Cruz. Secondary antibodies conjugated to appropriate fluorophores were obtained from Molecular Probes and Jackson Immunoresearch. AlexaFluor-conjugated phalloidin was purchased from Molecular Probes. Recombinant mouse ICAM-1-Fc, SDF-1α, and P-selectin were purchased from R&D Systems. The ROCK inhibitor Y-27632, the pan PI3K inhibitor LY-294002, and the PI3Kδ inhibitor IC87114 were obtained from CalBiochem. The myosin inhibitor (s)-nitro-blebbistatin was purchased from Cayman Chemicals. The actin destabilizing drug latrunculin B, the Src inhibitor PP2, the Abl kinase inhibitor STI-571, and the PI3Kγ inhibitor CZC24832 were purchased from Sigma.

Mice and cell culture

The mice used in the study (herein referred to as DKO) have been described previously (30). Crk fl/fl:CrkL fl/fl mice (49) (herein referred to as WT) were crossed with $CD4^+$ Cre mice to generate mice lacking the Crk and CrkL loci in T cells, starting at the double positive stage. Lifeact-GFP mice were described previously (104), and crossed with Crk fl/fl:CrkL fl/fl mice. The resulting Crk fl/fl:CrkL fl/fl lifeact-GFP mice were then crossed with $CD4^+$ Cre mice to generate DKO lifeact-GFP mice. Primary mouse $CD4^+$ T cells were purified from lymph nodes and spleens by negative selection. Briefly, after removing red blood cells by ACK lysis, cells were washed and incubated with anti-MHCII and anti-CD8 hybridoma supernatants (M5/114 and 2.43, respectively) for 20 min at 4°C. After washing, cells were mixed with anti-rat Ig magnetic beads (Qiagen BioMag), incubated for 15 min at 4°C, and

subjected to three rounds of magnetic separation using a bench top magnet. The resulting $CD4^+$ T cells were then immediately activated on 24-well plates coated with anti-CD3 and anti-CD28 (2C11 and PV1, 1μg/ml each) at 1×10^6 cells per well. Activation was done in T cell complete media, composed of DMEM (Gibco 11885–084) supplemented with 5% FBS, penicillin/streptomycin, non-essential amino acids, Glutamax, and 2μl 2-ME. Unless otherwise indicated, all tissue culture reagents were from Gibco. After 48h, cells were removed from activation and mixed at a 1:1 volume ratio with complete T cell media containing recombinant IL-2 (obtained through the NIH AIDS Reagent Program, Division of AIDS, NIAID, NIH from Dr. Maurice Gately, Hoffmann - La Roche Inc (105)), to give a final IL-2 concentration of 25 units/mL. T cells were used day 5–7 after activation.

Platinum-E (Plat-E) retroviral packaging cells were a kind gift from Dr. Michael Marks, Children's Hospital of Philadelphia, and were cultured in DMEM supplemented with 10% FBS, penicillin/streptomycin, and non-essential amino acids. For retroviral production, Plat-E cells were plated to 50% confluence on day 0. On day 1, cells were transfected with pMSCV encoding Grp1-PH-GFP (a kind gift from Dr. Morgan Huse, Sloan Kettering) using the calcium phosphate method. On day 2, the media was replaced, and on day 4 the virus-containing supernatant was harvested, aliquoted, and frozen at −80°C.

Static adhesion assays

96 well plates (MaxiSorp, ThermoFisher) were coated with 1μg/ml mouse ICAM-1 in PBS overnight at 4°C. Plates were then washed 3x with PBS, blocked with 1% BSA in PBS for 1h at RT, and washed twice with PBS. Activated $CD4^+$ T cells were used on days 5–7 after initial isolation. To prepare the cells, they were first labeled with Calcien AM (ThermoFisher) at a final concentration of 2.5μM for 30 min at 37°C in serum-free DMEM. Cells were then washed and resuspended in T cell complete media, and incubated at 37°C for 30 min. For Mn^{2+} treatment, the cells were then washed in HBS 1% BSA 10mM EDTA, washed again in HBS 1% BSA, and finally resuspended in HBS 2.5% BSA with 1mM Mn^{2+}. Otherwise, cells were resuspended in 2.5% BSA in PBS (with Ca^{2+} and Mg^{2+}). In each case, 1×10^5 cells were added to each well on ice in triplicate. After a 20 min incubation, the plate was read on a Bio-Tek Synergy HT fluorescence plate reader to obtain the baseline measurements representing "maximum adhesion" per well. Where indicated, PMA was added to a final concentration of 10ng/mL, and the plate was incubated at 37°C for 10 min, washed, and read again. The plate was washed and read a total of 2–4 times, until the signal from the unstimulated control was stable. To calculate the percent adhesion, the fluorescence per well after washes was divided by the initial "maximum adhesion" fluorescence reading per well. Background was subtracted using values obtained from empty wells.

Shear flow assays

Surfaces for analysis of T cell rolling and adhesion under shear flow conditions were prepared as described previously (106), with slight modifications. Ethanol cleaned gaskets were placed in the center of Corning 35mm dishes (430588), and the area was coated with 2μg/mL protein A/G (Pierce) and 1μg/mL SDF-1α and incubated overnight at 4°C. Surfaces were then washed 3x with PBS and incubated with 0.2μg/mL P-selectin and 1μg/mL

ICAM-1 for 3 hours at RT. Surfaces were then washed 3x with PBS followed by blocking in 1% BSA for 1 hour at RT. After 3 additional washes in PBS, surfaces were mounted onto a circular parallel-plate flow chamber (GlycoTech). The apparatus was mounted on a Zeiss Axiovert 200 microscope enclosed in a 37°C heated chamber equipped with a 10x A-Plan NA= 0.2 objective (Zeiss), and $CD4^+$ T cells were perfused into the chamber using a syringe pump (Harvard apparatus) at a flow rate corresponding to $100s^{-1}$. Videos were recorded continuously with a CCD camera (COHU 4195–4000) and DVD recorder at a rate of 30fps for 10 min. Using HandBrake and Quicktime software, the videos were converted into TIF format and loaded into ImageJ. Once in ImageJ, the images were processed by background subtraction and converted into binary images; cells were tracked using the plugin MTrack2. To restrict analysis to cells that are in close proximity to the surface, cells that flowed through the field in less than 3 seconds were thresholded out. A cell that remained immobile for 3 min or more was considered arrested, and cells with shorter bursts of surface interaction were considered rolling.

Measurement of cell spreading and F-actin responses

Activated $CD4^+$ T cells were resuspended in Ca^{2+} and Mg^{2+} free HBS (CMF-HBS), followed by a wash in CMF-HBS with 10mM EDTA. T cells were washed and resuspended in CMF-HBS, and incubated for 20min at 37°C. Cells were then adjusted to 0.5mM Ca^{2+} and 0.5mM Mg^{2+} (for control cells), or 1mM Mn^{2+} (for Mn^{2+} treatment), and then added to ICAM-1 coated coverslips (coated with 1μg/mL overnight at 4°C). After 20 min at 37°C, the cells were washed once in PBS containing Ca^{2+} and Mg^{2+} and fixed for 15 min in 3.7% PFA in PBS. Cells were then blocked and permeabilized in PBS, 0.01% saponin, 0.05% fish skin gelatin (PSG) for 20 min, followed by 45 min with fluorescent phalloidin (Molecular Probes) in PSG. Cells were washed 3x and mounted. For anti-CD3 stimulation, activated $CD4^+$ T cells were washed and resuspended in L15 media (Gibco) supplemented with 2mg/mL glucose and 1% FBS and allowed to interact with coverslips coated with 10μg/mL anti-CD3 clone 2C-11 alone, or anti-CD3 and 2μg/mL ICAM-1. After 20 min at 37°C, the cells were washed once in PBS containing Ca^{2+} and Mg^{2+} and fixed for 15 min in 3.7% PFA in PBS. Cells were then blocked and permeabilized in PSG for 20 min, followed by 45 min with fluorescent phalloidin in PSG. Cells were washed 3x, mounted, and imaged using a 63x PlanApo 1.4 NA objective on an Axiovert 200M (Zeiss) with a spinning disk confocal system (Ultraview ERS6; PerkinElmer). Three z-planes spanning 0.5μm were collected at the cell-surface interface with an Orca ER camera (Hamamatsu). Image analysis was conducted using Velocity v6.3 software. Cells were identified using the “Find Objects” command, using a low threshold on the actin channel, and total phalloidin staining was quantified per cell based on integrated pixel intensity.

PIP_3 Visualization

Freshly isolated $CD4^+$ T cells were plated with 25 U/mL IL-2 in 24-well plates pre-coated with 1μg/ml 2C-11 and PV1. After 48 hrs, cells were harvested, centrifuged and resuspended in viral supernatants. Cells were then spinocculated by centrifugation for 2 hours at 1200g at 37°C. Cells were then cultured with 25 U/mL IL-2, and used on day 5 after initial harvest. For imaging, Lab-Tek 8 chamber slides (ThermoFisher) were coated with 2μg/mL ICAM-1 overnight at 4°C. $CD4^+$ T cells were washed and resuspended in L15 media (Gibco)

supplemented with 2mg/mL glucose, and added to the chambers. After 20 min, chambers were gently washed to remove unbound cells, then imaged using the confocal system described above. Image analysis and preparation was done using Velocity v6.3 and ImageJ software. Briefly, T cells were divided into thirds, and the mean fluorescence intensity of the membrane edge of the front third and the rear third was determined. Data is displayed as the ratio of the front third to the rear third, which corresponds to relative enrichment of PIP_3.

Migration on ICAM-1

Lab-Tek 8 chamber slides (ThermoFisher) were coated with 2μg/mL ICAM-1 overnight at 4°C. Activated $CD4^+$ T cells were washed and resuspended in L15 media (Gibco) supplemented with 2mg/mL glucose and 1% FBS. T cells were then added to the chambers, incubated 20 min, gently washed to remove all unbound cells, and imaged using a 10x Phase objective at 37°C on a Zeiss Axiovert 200M inverted microscope equipped with an MS-2000 automatic stage (Applied Scientific Instruments) and a Roper Scientific EMCCD camera. Time lapse imaging was performed using SlideBook 6 software (Intelligent Imaging Innovations, Inc.), collecting one image every 30 sec for 10 min total. For drug treatments, the indicated drug was added and pre-incubated 5 min before imaging. Movies were exported into ImageJ, and cells were tracked using the manual tracking plugin. Directionality was calculated in Excel by dividing net displacement by total track length for each cell. Cells were scored as motile if they showed a polarized morphology and migrated at least 3 cell diameters. For higher magnification movies, cells were imaged every 5 sec for 3–5 min using a 63x objective.

Biochemical analysis of cell signaling in response to surface-bound ICAM-1

60mm dishes (Corning, 430166) were coated with 2μg/mL ICAM-1 overnight at 4°C. Activated $CD4^+$ T cells were serum starved for 3 hours in DMEM, washed and resuspended in CMF-HBS, followed by a wash in CMF-HBS containing 10mM EDTA. T cells were then washed and resuspended in CMF-HBS, and incubated for 20 min at 37°C. T cells were then treated with Ca^{2+} and Mg^{2+} (unstimulated control), or treated with Mn^{2+} alone or together with 1μg/mL soluble ICAM-1, or treated with Mn^{2+} and allowed to interact with surface bound ICAM-1. After 20 min at 37°C, cells stimulated in solution were lysed by adding 2x ice cold lysis buffer (Final lysis buffer composition: 1% Triton X-100, 150mM NaCl, 50mM HEPES, 10mM $MgCl_2$, 5mM NaF, 1mM sodium orthovanadate, and Roche EDTA-free protease inhibitor cocktail). Cell stimulated on surface-bound ICAM-1 were lysed by aspirating the media and adding 1x ice cold lysis buffer. Lysates were incubated on ice with periodic vortexing for 20 min, followed by centrifugation for 10 min at 16,000g at 4°C. Lysates were used for immunoprecipitations and GST-pulldowns (see below). A small aliquot of each whole cell lysate was retained, mixed with 4x sample buffer containing DTT (50mM final), and heated to 95°C for 10 min prior to separation by SDS-PAGE.

Immunoprecipitation

Protein A agarose beads (Repligen) were washed and resupended in lysis buffer. Beads were then bound to either anti-phosphotyrosine (PY-20, 2.5μg per condition), anti-p85 (5μg per condition), or anti-CrkL (1μg per condition) overnight at 4°C, with rotation. Beads were then

washed 3x times with lysis buffer, mixed with cell lysates, and rotated at 4°C overnight. Beads were then washed 3x and mixed with sample buffer for SDS-PAGE.

GTPase Pulldowns

GTP bound GTPases were isolated as in (107). Briefly, GST-PAK PBD (a kind gift from Dr. Keith Burridge) was expressed in *E.coli* strain BL21(DE3), conjugated to glutathione sepharose 4B beads (GE Healthcare) and stored for up to two weeks at 4°C. Cell lysates were mixed with the GST-PAK PBD beads for 45 min rotating at 4°C, followed by two washes with 1x ice cold lysis buffer, and resuspended in sample buffer for SDS-PAGE.

Western Blotting

Western blotting was performed using the Invitrogen Novex Mini-cell system with NuPAGE 4–12% BisTris gels. Proteins were transferred to nitrocellulose membranes (0.45μm, BioRad) and blocked using LI-COR blocking buffer at a 1:1 with PBS for 1 hr at RT. Primary antibodies were mixed in TBS 0.1% tween-20 (TBST) with 2% BSA and incubated with membranes overnight at 4°C on a shaker. Membranes were then washed 3× 10 min in TBST, and incubated with fluorophore-conjugated secondary antibodies in TBST with 2% BSA for 1 hr at RT. Membranes were washed 3× 10 min in TBST, and imaged using a LI-COR Odyssey imaging system. Quantification of bands was done using ImageStudio software (LI-COR).

T cell stimulation on hydrogels

Polyacrylamide hydrogels were purchased from Matrigen. For ICAM-1 coating, hydrogels were washed in PBS and incubated with 6μg/ml ICAM-1 in PBS for 2 hours at RT. Hydrogels were then washed 3× 5 min in PBS, blocked with 1% BSA in PBS for 1 hour at RT, and washed with PBS. To measure F-actin responses, activated $CD4^+$ T cells were resuspended in CMF-HBS, followed by a wash in CMF-HBS with 10mM EDTA. T cells were then washed and resuspended in CMF-HBS and incubated for 20 min at 37°C. T cells were then treated with 1mM Mn^{2+}, and added to ICAM-1 coated hydrogels (Softview imaging dishes). Cells were fixed and phalloidin labeled, and F-actin abundance was determined as described above. For biochemical analysis, $CD4^+$ T cells were serum starved for 3 hrs in DMEM, washed and resuspended in CMF-HBS, followed by a wash in CMF-HBS with 10mM EDTA. T cells were then washed and resuspended in CMF-HBS, and incubated for 20 min at 37°C. T cells were then treated with 1mM Mn^{2+}, and added to ICAM-1 coated hydrogels (Softwell 6-well plates). After 20 min at 37°C, cells were lysed by aspirating the media and adding 1x ice cold lysis buffer. Lysates were analyzed as described above.

Statistical analysis

Statistics were calculated and graphs were prepared using GraphPad Prism 7. When only two groups were being compared, a t-test was used. When more than two groups were compared, a one-way ANOVA was performed using multiple comparisons with a Tukey correction. When data was not normal, a transformation was performed followed by analysis using a one-way ANOVA on the normalized data. *$p<0.05$; **$p<0.01$; ***$p<0.001$

Supplementary Material

Refer to Web version on PubMed Central for supplementary material.

Acknowledgments:

We would like to thank all members of the Burkhardt lab for useful discussions and critical reading of the manuscript. Special thanks to Dr. Steven Seeholzer and Lynn Spruce in the CHOP protein and proteomics core facility for expert assistance with mass spectrometry. We also thank Dr. Morgan Huse (Memorial Sloan Kettering) for providing the GFP labeled GRP1 PH domain, Dr. Michael Marks (CHOP) for providing the Platinum-E cells, and Dr. Keith Burridge (Univ. North Carolina) for provided the GST-PAK-PBD construct.

Funding: Funding for this work was provided by the National Institutes of Health (NIH) in grants R01 HL128551 and R01 GM104867 to JKB; T32 TCA009140 to NHR; R01 AI082292, R01 HL18208, and R01 GM123019 to DAH; F32 GM110961 to JLM; and R21 AI32828 to JKB. NHR is also a Cancer Research Institute Irvington Fellow supported by the Cancer Research Institute.

References

1. Denucci CC, Mitchell JS, Shimizu Y. 2009 Integrin function in T-cell homing to lymphoid and nonlymphoid sites: getting there and staying there. Crit Rev Immunol 29:87–109. [PubMed: 19496742]
2. Nourshargh S, Alon R. 2014 Leukocyte migration into inflamed tissues. Immunity 41:694–707. [PubMed: 25517612]
3. Roman MJ, Devereux RB, Schwartz JE, Lockshin MD, Paget SA, Davis A, Crow MK, Sammaritano L, Levine DM, Shankar BA, Moeller E, Salmon JE. 2005 Arterial stiffness in chronic inflammatory diseases. Hypertension 46:194–199. [PubMed: 15911740]
4. Tracqui P, Broisat A, Toczek J, Mesnier N, Ohayon J, Riou L. 2011 Mapping elasticity moduli of atherosclerotic plaque in situ via atomic force microscopy. J Struct Biol 174:115–123. [PubMed: 21296163]
5. Huveneers S, Daemen MJ, Hordijk PL. 2015 Between Rho(k) and a hard place: the relation between vessel wall stiffness, endothelial contractility, and cardiovascular disease. Circ Res 116:895–908. [PubMed: 25722443]
6. Stroka KM, Aranda-Espinoza H. 2011 Endothelial cell substrate stiffness influences neutrophil transmigration via myosin light chain kinase-dependent cell contraction. Blood 118:1632–1640. [PubMed: 21652678]
7. Huynh J, Nishimura N, Rana K, Peloquin JM, Califano JP, Montague CR, King MR, Schaffer CB, Reinhart-King CA. 2011 Age-related intimal stiffening enhances endothelial permeability and leukocyte transmigration. Sci Transl Med 3:112ra122.
8. Steiner O, Coisne C, Cecchelli R, Boscacci R, Deutsch U, Engelhardt B, Lyck R. 2010 Differential roles for endothelial ICAM-1, ICAM-2, and VCAM-1 in shear-resistant T cell arrest, polarization, and directed crawling on blood-brain barrier endothelium. J Immunol 185:4846–4855. [PubMed: 20861356]
9. Schenkel AR, Mamdouh Z, Muller WA. 2004 Locomotion of monocytes on endothelium is a critical step during extravasation. Nat Immunol 5:393–400. [PubMed: 15021878]
10. Phillipson M, Heit B, Colarusso P, Liu L, Ballantyne CM, Kubes P. 2006 Intraluminal crawling of neutrophils to emigration sites: a molecularly distinct process from adhesion in the recruitment cascade. J Exp Med 203:2569–2575. [PubMed: 17116736]
11. Bartholomaus I, Kawakami N, Odoardi F, Schlager C, Miljkovic D, Ellwart JW, Klinkert WE, Flugel-Koch C, Issekutz TB, Wekerle H, Flugel A. 2009 Effector T cell interactions with meningeal vascular structures in nascent autoimmune CNS lesions. Nature 462:94–98. [PubMed: 19829296]
12. Gorina R, Lyck R, Vestweber D, Engelhardt B. 2014 beta2 integrin-mediated crawling on endothelial ICAM-1 and ICAM-2 is a prerequisite for transcellular neutrophil diapedesis across the inflamed blood-brain barrier. J Immunol 192:324–337. [PubMed: 24259506]

13. Kelleher D, Murphy A, Cullen D. 1990 Leukocyte function-associated antigen 1 (LFA-1) is a signaling molecule for cytoskeletal changes in a human T cell line. Eur J Immunol 20:2351–2354. [PubMed: 2242762]
14. Porter JC, Bracke M, Smith A, Davies D, Hogg N. 2002 Signaling through integrin LFA-1 leads to filamentous actin polymerization and remodeling, resulting in enhanced T cell adhesion. J Immunol 168:6330–6335. [PubMed: 12055249]
15. Smith A, Bracke M, Leitinger B, Porter JC, Hogg N. 2003 LFA-1-induced T cell migration on ICAM-1 involves regulation of MLCK-mediated attachment and ROCK-dependent detachment. J Cell Sci 116:3123–3133. [PubMed: 12799414]
16. Eyckmans J, Boudou T, Yu X, Chen CS. 2011 A hitchhiker's guide to mechanobiology. Dev Cell 21:35–47. [PubMed: 21763607]
17. Sun Z, Guo SS, Fassler R. 2016 Integrin-mediated mechanotransduction. J Cell Biol 215:445–456. [PubMed: 27872252]
18. Luo BH, Carman CV, Springer TA. 2007 Structural basis of integrin regulation and signaling. Annu Rev Immunol 25:619–647. [PubMed: 17201681]
19. Hogg N, Patzak I, Willenbrock F. 2011 The insider's guide to leukocyte integrin signalling and function. Nat Rev Immunol 11:416–426. [PubMed: 21597477]
20. Alon R, Shulman Z. 2011 Chemokine triggered integrin activation and actin remodeling events guiding lymphocyte migration across vascular barriers. Exp Cell Res 317:632–641. [PubMed: 21376176]
21. Abram CL, Lowell CA. 2009 The ins and outs of leukocyte integrin signaling. Annu Rev Immunol 27:339–362. [PubMed: 19302044]
22. Verma NK, Kelleher D. 2014 Adaptor regulation of LFA-1 signaling in T lymphocyte migration: Potential druggable targets for immunotherapies? Eur J Immunol 44:3484–3499. [PubMed: 25251823]
23. Kliche S, Breitling D, Togni M, Pusch R, Heuer K, Wang X, Freund C, Kasirer-Friede A, Menasche G, Koretzky GA, Schraven B. 2006 The ADAP/SKAP55 signaling module regulates T-cell receptor-mediated integrin activation through plasma membrane targeting of Rap1. Mol Cell Biol 26:7130–7144. [PubMed: 16980616]
24. Suzuki J, Yamasaki S, Wu J, Koretzky GA, Saito T. 2007 The actin cloud induced by LFA-1-mediated outside-in signals lowers the threshold for T-cell activation. Blood 109:168–175. [PubMed: 16973965]
25. Wang H, Wei B, Bismuth G, Rudd CE. 2009 SLP-76-ADAP adaptor module regulates LFA-1 mediated costimulation and T cell motility. Proc Natl Acad Sci U S A 106:12436–12441. [PubMed: 19617540]
26. Nieves B, Jones CW, Ward R, Ohta Y, Reverte CG, LaFlamme SE. 2010 The NPIY motif in the integrin beta1 tail dictates the requirement for talin-1 in outside-in signaling. J Cell Sci 123:1216–1226. [PubMed: 20332112]
27. Hyduk SJ, Rullo J, Cano AP, Xiao H, Chen M, Moser M, Cybulsky MI. 2011 Talin-1 and kindlin-3 regulate alpha4beta1 integrin-mediated adhesion stabilization, but not G protein-coupled receptor-induced affinity upregulation. J Immunol 187:4360–4368. [PubMed: 21911599]
28. Bledzka K, Bialkowska K, Sossey-Alaoui K, Vaynberg J, Pluskota E, Qin J, Plow EF. 2016 Kindlin-2 directly binds actin and regulates integrin outside-in signaling. J Cell Biol 213:97–108. [PubMed: 27044892]
29. Nolz JC, Nacusi LP, Segovis CM, Medeiros RB, Mitchell JS, Shimizu Y, Billadeau DD. 2008 The WAVE2 complex regulates T cell receptor signaling to integrins via Abl- and CrkL-C3G-mediated activation of Rap1. J Cell Biol 182:1231–1244. [PubMed: 18809728]
30. Huang Y, Clarke F, Karimi M, Roy NH, Williamson EK, Okumura M, Mochizuki K, Chen EJ, Park TJ, Debes GF, Zhang Y, Curran T, Kambayashi T, Burkhardt JK. 2015 CRK proteins selectively regulate T cell migration into inflamed tissues. J Clin Invest 125:1019–1032. [PubMed: 25621495]
31. Guris DL, Fantes J, Tara D, Druker BJ, Imamoto A. 2001 Mice lacking the homologue of the human 22q11.2 gene CRKL phenocopy neurocristopathies of DiGeorge syndrome. Nat Genet 27:293–298. [PubMed: 11242111]

32. Park TJ, Boyd K, Curran T. 2006 Cardiovascular and craniofacial defects in Crk-null mice. Mol Cell Biol 26:6272–6282. [PubMed: 16880535]
33. Li L, Guris DL, Okura M, Imamoto A. 2003 Translocation of CrkL to focal adhesions mediates integrin-induced migration downstream of Src family kinases. Mol Cell Biol 23:2883–2892. [PubMed: 12665586]
34. Antoku S, Mayer BJ. 2009 Distinct roles for Crk adaptor isoforms in actin reorganization induced by extracellular signals. J Cell Sci 122:4228–4238. [PubMed: 19861495]
35. Watanabe T, Tsuda M, Makino Y, Konstantinou T, Nishihara H, Majima T, Minami A, Feller SM, Tanaka S. 2009 Crk adaptor protein-induced phosphorylation of Gab1 on tyrosine 307 via Src is important for organization of focal adhesions and enhanced cell migration. Cell Res 19:638–650. [PubMed: 19350053]
36. Park TJ, Curran T. 2014 Essential roles of Crk and CrkL in fibroblast structure and motility. Oncogene 33:5121–5132. [PubMed: 24166500]
37. Feller SM. 2001 Crk family adaptors-signalling complex formation and biological roles. Oncogene 20:6348–6371. [PubMed: 11607838]
38. Chodniewicz D, Klemke RL. 2004 Regulation of integrin-mediated cellular responses through assembly of a CAS/Crk scaffold. Biochim Biophys Acta 1692:63–76. [PubMed: 15246680]
39. Tsuda M, Tanaka S. 2012 Roles for crk in cancer metastasis and invasion. Genes Cancer 3:334–340. [PubMed: 23226571]
40. Kumar S, Fajardo JE, Birge RB, Sriram G. 2014 Crk at the quarter century mark: perspectives in signaling and cancer. J Cell Biochem 115:819–825. [PubMed: 24356912]
41. Dransfield I, Cabanas C, Craig A, Hogg N. 1992 Divalent cation regulation of the function of the leukocyte integrin LFA-1. J Cell Biol 116:219–226. [PubMed: 1346139]
42. Jacobelli J, Bennett FC, Pandurangi P, Tooley AJ, Krummel MF. 2009 Myosin-IIA and ICAM-1 regulate the interchange between two distinct modes of T cell migration. J Immunol 182:2041–2050. [PubMed: 19201857]
43. Jacobelli J, Friedman RS, Conti MA, Lennon-Dumenil AM, Piel M, Sorensen CM, Adelstein RS, Krummel MF. 2010 Confinement-optimized three-dimensional T cell amoeboid motility is modulated via myosin IIA-regulated adhesions. Nat Immunol 11:953–961. [PubMed: 20835229]
44. Labno CM, Lewis CM, You D, Leung DW, Takesono A, Kamberos N, Seth A, Finkelstein LD, Rosen MK, Schwartzberg PL, Burkhardt JK. 2003 Itk functions to control actin polymerization at the immune synapse through localized activation of Cdc42 and WASP. Curr Biol 13:1619–1624. [PubMed: 13678593]
45. Akagi T, Shishido T, Murata K, Hanafusa H. 2000 v-Crk activates the phosphoinositide 3-kinase/AKT pathway in transformation. Proc Natl Acad Sci U S A 97:7290–7295. [PubMed: 10852971]
46. Akagi T, Murata K, Shishido T, Hanafusa H. 2002 v-Crk activates the phosphoinositide 3-kinase/AKT pathway by utilizing focal adhesion kinase and H-Ras. Mol Cell Biol 22:7015–7023. [PubMed: 12242282]
47. Stam JC, Geerts WJ, Versteeg HH, Verkleij AJ, van Bergen en Henegouwen PM. 2001 The v-Crk oncogene enhances cell survival and induces activation of protein kinase B/Akt. J Biol Chem 276:25176–25183. [PubMed: 11323409]
48. Salameh A, Galvagni F, Bardelli M, Bussolino F, Oliviero S. 2005 Direct recruitment of CRK and GRB2 to VEGFR-3 induces proliferation, migration, and survival of endothelial cells through the activation of ERK, AKT, and JNK pathways. Blood 106:3423–3431. [PubMed: 16076871]
49. Park TJ, Curran T. 2008 Crk and Crk-like play essential overlapping roles downstream of disabled-1 in the Reelin pathway. J Neurosci 28:13551–13562. [PubMed: 19074029]
50. Cheng S, Guo J, Yang Q, Han L. 2015 Crk-like adapter protein is required for TGF-beta-induced AKT and ERK-signaling pathway in epithelial ovarian carcinomas. Tumour Biol 36:915–919. [PubMed: 25307974]
51. Cain RJ, Ridley AJ. 2009 Phosphoinositide 3-kinases in cell migration. Biol Cell 101:13–29. [PubMed: 19055486]

52. Kavran JM, Klein DE, Lee A, Falasca M, Isakoff SJ, Skolnik EY, Lemmon MA. 1998 Specificity and promiscuity in phosphoinositide binding by pleckstrin homology domains. J Biol Chem 273:30497–30508. [PubMed: 9804818]
53. Beinke S, Phee H, Clingan JM, Schlessinger J, Matloubian M, Weiss A. 2010 Proline-rich tyrosine kinase-2 is critical for CD8 T-cell short-lived effector fate. Proc Natl Acad Sci U S A 107:16234–16239. [PubMed: 20805505]
54. Cheung SM, Ostergaard HL. 2016 Pyk2 Controls Integrin-Dependent CTL Migration through Regulation of De-Adhesion. J Immunol 197:1945–1956. [PubMed: 27456486]
55. Sawada Y, Tamada M, Dubin-Thaler BJ, Cherniavskaya O, Sakai R, Tanaka S, Sheetz MP. 2006 Force sensing by mechanical extension of the Src family kinase substrate p130Cas. Cell 127:1015–1026. [PubMed: 17129785]
56. Kumari S, Vardhana S, Cammer M, Curado S, Santos L, Sheetz MP, Dustin ML. 2012 T Lymphocyte Myosin IIA is Required for Maturation of the Immunological Synapse. Front Immunol 3:230. [PubMed: 22912631]
57. Yu Y, Fay NC, Smoligovets AA, Wu HJ, Groves JT. 2012 Myosin IIA modulates T cell receptor transport and CasL phosphorylation during early immunological synapse formation. PLoS One 7:e30704. [PubMed: 22347397]
58. Santos LC, Blair DA, Kumari S, Cammer M, Iskratsch T, Herbin O, Alexandropoulos K, Dustin ML, Sheetz MP. 2016 Actin polymerization-dependent activation of Cas-L promotes immunological synapse stability. Immunol Cell Biol doi:10.1038/icb.2016.61.
59. Sato T, Tachibana K, Nojima Y, D'Avirro N, Morimoto C. 1995 Role of the VLA-4 molecule in T cell costimulation. Identification of the tyrosine phosphorylation pattern induced by the ligation of VLA-4. J Immunol 155:2938–2947. [PubMed: 7673711]
60. Hunter AJ, Shimizu Y. 1997 Alpha 4 beta 1 integrin-mediated tyrosine phosphorylation in human T cells: characterization of Crk- and Fyn-associated substrates (pp105, pp115, and human enhancer of filamentation-1) and integrin-dependent activation of p59fyn1. J Immunol 159:4806–4814. [PubMed: 9366405]
61. Naramura M, Kole HK, Hu RJ, Gu H. 1998 Altered thymic positive selection and intracellular signals in Cbl-deficient mice. Proc Natl Acad Sci U S A 95:15547–15552. [PubMed: 9861006]
62. Murphy MA, Schnall RG, Venter DJ, Barnett L, Bertoncello I, Thien CB, Langdon WY, Bowtell DD. 1998 Tissue hyperplasia and enhanced T-cell signalling via ZAP-70 in c-Cbl-deficient mice. Mol Cell Biol 18:4872–4882. [PubMed: 9671496]
63. Thien CB, Bowtell DD, Langdon WY. 1999 Perturbed regulation of ZAP-70 and sustained tyrosine phosphorylation of LAT and SLP-76 in c-Cbl-deficient thymocytes. J Immunol 162:7133–7139. [PubMed: 10358158]
64. Rao N, Lupher ML Jr., Ota S, Reedquist KA, Druker BJ, Band H. 2000 The linker phosphorylation site Tyr292 mediates the negative regulatory effect of Cbl on ZAP-70 in T cells. J Immunol 164:4616–4626. [PubMed: 10779765]
65. Thien CB, Blystad FD, Zhan Y, Lew AM, Voigt V, Andoniou CE, Langdon WY. 2005 Loss of c-Cbl RING finger function results in high-intensity TCR signaling and thymic deletion. EMBO J 24:3807–3819. [PubMed: 16211006]
66. Balagopalan L, Barr VA, Sommers CL, Barda-Saad M, Goyal A, Isakowitz MS, Samelson LE. 2007 c-Cbl-mediated regulation of LAT-nucleated signaling complexes. Mol Cell Biol 27:8622–8636. [PubMed: 17938199]
67. Langdon WY, Hartley JW, Klinken SP, Ruscetti SK, Morse HC 3rd. 1989 v-cbl, an oncogene from a dual-recombinant murine retrovirus that induces early B-lineage lymphomas. Proc Natl Acad Sci U S A 86:1168–1172. [PubMed: 2784003]
68. Ribon V, Hubbell S, Herrera R, Saltiel AR. 1996 The product of the cbl oncogene forms stable complexes in vivo with endogenous Crk in a tyrosine phosphorylation-dependent manner. Mol Cell Biol 16:45–52. [PubMed: 8524328]
69. Sattler M, Salgia R, Okuda K, Uemura N, Durstin MA, Pisick E, Xu G, Li JL, Prasad KV, Griffin JD. 1996 The proto-oncogene product p120CBL and the adaptor proteins CRKL and c-CRK link c-ABL, p190BCR/ABL and p210BCR/ABL to the phosphatidylinositol-3' kinase pathway. Oncogene 12:839–846. [PubMed: 8632906]

70. Jain SK, Langdon WY, Varticovski L. 1997 Tyrosine phosphorylation of p120cbl in BCR/abl transformed hematopoietic cells mediates enhanced association with phosphatidylinositol 3-kinase. Oncogene 14:2217–2228. [PubMed: 9174058]
71. Ni HT, Deeths MJ, Mescher MF. 2001 LFA-1-mediated costimulation of CD8+ T cell proliferation requires phosphatidylinositol 3-kinase activity. J Immunol 166:6523–6529. [PubMed: 11359803]
72. Sanchez-Martin L, Sanchez-Sanchez N, Gutierrez-Lopez MD, Rojo AI, Vicente-Manzanares M, Perez-Alvarez MJ, Sanchez-Mateos P, Bustelo XR, Cuadrado A, Sanchez-Madrid F, Rodriguez-Fernandez JL, Cabanas C. 2004 Signaling through the leukocyte integrin LFA-1 in T cells induces a transient activation of Rac-1 that is regulated by Vav and PI3K/Akt-1. J Biol Chem 279:16194–16205. [PubMed: 14960575]
73. Verma NK, Fazil MH, Ong ST, Chalasani ML, Low JH, Kottaiswamy A, P P, Kizhakeyil A, Kumar S, Panda AK, Freeley M, Smith SM, Boehm BO, Kelleher D. 2016 LFA-1/ICAM-1 Ligation in Human T Cells Promotes Th1 Polarization through a GSK3beta Signaling-Dependent Notch Pathway. J Immunol 197:108–118. [PubMed: 27206767]
74. Meng F, Lowell CA. 1998 A beta 1 integrin signaling pathway involving Src-family kinases, Cbl and PI-3 kinase is required for macrophage spreading and migration. EMBO J 17:4391–4403. [PubMed: 9687507]
75. Jankowski W, Saleh T, Pai MT, Sriram G, Birge RB, Kalodimos CG. 2012 Domain organization differences explain Bcr-Abl's preference for CrkL over CrkII. Nat Chem Biol 8:590–596. [PubMed: 22581121]
76. Lemmon MA, Ferguson KM, Abrams CS. 2002 Pleckstrin homology domains and the cytoskeleton. FEBS Lett 513:71–76. [PubMed: 11911883]
77. Akakura S, Kar B, Singh S, Cho L, Tibrewal N, Sanokawa-Akakura R, Reichman C, Ravichandran KS, Birge RB. 2005 C-terminal SH3 domain of CrkII regulates the assembly and function of the DOCK180/ELMO Rac-GEF. J Cell Physiol 204:344–351. [PubMed: 15700267]
78. Albert ML, Kim JI, Birge RB. 2000 alphavbeta5 integrin recruits the CrkII-Dock180-rac1 complex for phagocytosis of apoptotic cells. Nat Cell Biol 2:899–905. [PubMed: 11146654]
79. Nishihara H, Maeda M, Oda A, Tsuda M, Sawa H, Nagashima K, Tanaka S. 2002 DOCK2 associates with CrkL and regulates Rac1 in human leukemia cell lines. Blood 100:3968–3974. [PubMed: 12393632]
80. Renkawitz J, Sixt M. 2010 Mechanisms of force generation and force transmission during interstitial leukocyte migration. EMBO Rep 11:744–750. [PubMed: 20865016]
81. Lammermann T, Germain RN. 2014 The multiple faces of leukocyte interstitial migration. Semin Immunopathol 36:227–251. [PubMed: 24573488]
82. Case LB, Waterman CM. 2015 Integration of actin dynamics and cell adhesion by a three-dimensional, mechanosensitive molecular clutch. Nat Cell Biol 17:955–963. [PubMed: 26121555]
83. Tamada M, Sheetz MP, Sawada Y. 2004 Activation of a signaling cascade by cytoskeleton stretch. Dev Cell 7:709–718. [PubMed: 15525532]
84. Kostic A, Sheetz MP. 2006 Fibronectin rigidity response through Fyn and p130Cas recruitment to the leading edge. Mol Biol Cell 17:2684–2695. [PubMed: 16597701]
85. Alexander NR, Branch KM, Parekh A, Clark ES, Iwueke IC, Guelcher SA, Weaver AM. 2008 Extracellular matrix rigidity promotes invadopodia activity. Curr Biol 18:1295–1299. [PubMed: 18718759]
86. Zhang X, Moore SW, Iskratsch T, Sheetz MP. 2014 N-WASP-directed actin polymerization activates Cas phosphorylation and lamellipodium spreading. J Cell Sci 127:1394–1405. [PubMed: 24481817]
87. Carman CV, Sage PT, Sciuto TE, de la Fuente MA, Geha RS, Ochs HD, Dvorak HF, Dvorak AM, Springer TA. 2007 Transcellular diapedesis is initiated by invasive podosomes. Immunity 26:784–797. [PubMed: 17570692]
88. Shulman Z, Shinder V, Klein E, Grabovsky V, Yeger O, Geron E, Montresor A, Bolomini-Vittori M, Feigelson SW, Kirchhausen T, Laudanna C, Shakhar G, Alon R. 2009 Lymphocyte crawling and transendothelial migration require chemokine triggering of high-affinity LFA-1 integrin. Immunity 30:384–396. [PubMed: 19268609]

89. Martinelli R, Zeiger AS, Whitfield M, Sciuto TE, Dvorak A, Van Vliet KJ, Greenwood J, Carman CV. 2014 Probing the biomechanical contribution of the endothelium to lymphocyte migration: diapedesis by the path of least resistance. J Cell Sci 127:3720–3734. [PubMed: 25002404]

90. Laurent S, Boutouyrie P. 2007 Recent advances in arterial stiffness and wave reflection in human hypertension. Hypertension 49:1202–1206. [PubMed: 17452508]

91. Carrera AC, Rincon M, Sanchez-Madrid F, Lopez-Botet M, de Landazuri MO. 1988 Triggering of co-mitogenic signals in T cell proliferation by anti-LFA-1 (CD18, CD11a), LFA-3, and CD7 monoclonal antibodies. J Immunol 141:1919–1924. [PubMed: 2459196]

92. Van Seventer GA, Shimizu Y, Horgan KJ, Shaw S. 1990 The LFA-1 ligand ICAM-1 provides an important costimulatory signal for T cell receptor-mediated activation of resting T cells. J Immunol 144:4579–4586. [PubMed: 1972160]

93. Buday L, Khwaja A, Sipeki S, Farago A, Downward J. 1996 Interactions of Cbl with two adapter proteins, Grb2 and Crk, upon T cell activation. J Biol Chem 271:6159–6163. [PubMed: 8626404]

94. Reedquist KA, Fukazawa T, Panchamoorthy G, Langdon WY, Shoelson SE, Druker BJ, Band H. 1996 Stimulation through the T cell receptor induces Cbl association with Crk proteins and the guanine nucleotide exchange protein C3G. J Biol Chem 271:8435–8442. [PubMed: 8626543]

95. Sawasdikosol S, Chang JH, Pratt JC, Wolf G, Shoelson SE, Burakoff SJ. 1996 Tyrosine-phosphorylated Cbl binds to Crk after T cell activation. J Immunol 157:110–116. [PubMed: 8683103]

96. van Leeuwen JE, Paik PK, Samelson LE. 1999 Activation of nuclear factor of activated T cells-(NFAT) and activating protein 1 (AP-1) by oncogenic 70Z Cbl requires an intact phosphotyrosine binding domain but not Crk(L) or p85 phosphatidylinositol 3-kinase association. J Biol Chem 274:5153–5162. [PubMed: 9988765]

97. Gelkop S, Babichev Y, Isakov N. 2001 T cell activation induces direct binding of the Crk adapter protein to the regulatory subunit of phosphatidylinositol 3-kinase (p85) via a complex mechanism involving the Cbl protein. J Biol Chem 276:36174–36182. [PubMed: 11418612]

98. Azoulay-Alfaguter I, Strazza M, Peled M, Novak HK, Muller J, Dustin ML, Mor A. 2017 The tyrosine phosphatase SHP-1 promotes T cell adhesion by activating the adaptor protein CrkII in the immunological synapse. Sci Signal 10.

99. Kumari S, Depoil D, Martinelli R, Judokusumo E, Carmona G, Gertler FB, Kam LC, Carman CV, Burkhardt JK, Irvine DJ, Dustin ML. 2015 Actin foci facilitate activation of the phospholipase C-gamma in primary T lymphocytes via the WASP pathway. Elife 4.

100. O'Connor RS, Hao X, Shen K, Bashour K, Akimova T, Hancock WW, Kam LC, Milone MC. 2012 Substrate rigidity regulates human T cell activation and proliferation. J Immunol 189:1330–1339. [PubMed: 22732590]

101. Judokusumo E, Tabdanov E, Kumari S, Dustin ML, Kam LC. 2012 Mechanosensing in T lymphocyte activation. Biophys J 102:L5–7. [PubMed: 22339876]

102. Saitakis M, Dogniaux S, Goudot C, Bufi N, Asnacios S, Maurin M, Randriamampita C, Asnacios A, Hivroz C. 2017 Different TCR-induced T lymphocyte responses are potentiated by stiffness with variable sensitivity. Elife 6.

103. Lambert LH, Goebrecht GK, De Leo SE, O'Connor RS, Nunez-Cruz S, Li TD, Yuan J, Milone MC, Kam LC. 2017 Improving T Cell Expansion with a Soft Touch. Nano Lett 17:821–826. [PubMed: 28122453]

104. Riedl J, Flynn KC, Raducanu A, Gartner F, Beck G, Bosl M, Bradke F, Massberg S, Aszodi A, Sixt M, Wedlich-Soldner R. 2010 Lifeact mice for studying F-actin dynamics. Nat Methods 7:168–169. [PubMed: 20195247]

105. Lahm HW, Stein S. 1985 Characterization of recombinant human interleukin-2 with micromethods. J Chromatogr 326:357–361. [PubMed: 3875623]

106. Lee D, Kim J, Beste MT, Koretzky GA, Hammer DA. 2012 Diacylglycerol kinase zeta negatively regulates CXCR4-stimulated T lymphocyte firm arrest to ICAM-1 under shear flow. Integr Biol (Camb) 4:606–614. [PubMed: 22546945]

107. Huang Y, Comiskey EO, Dupree RS, Li S, Koleske AJ, Burkhardt JK. 2008 The c-Abl tyrosine kinase regulates actin remodeling at the immune synapse. Blood 112:111–119. [PubMed: 18305217]

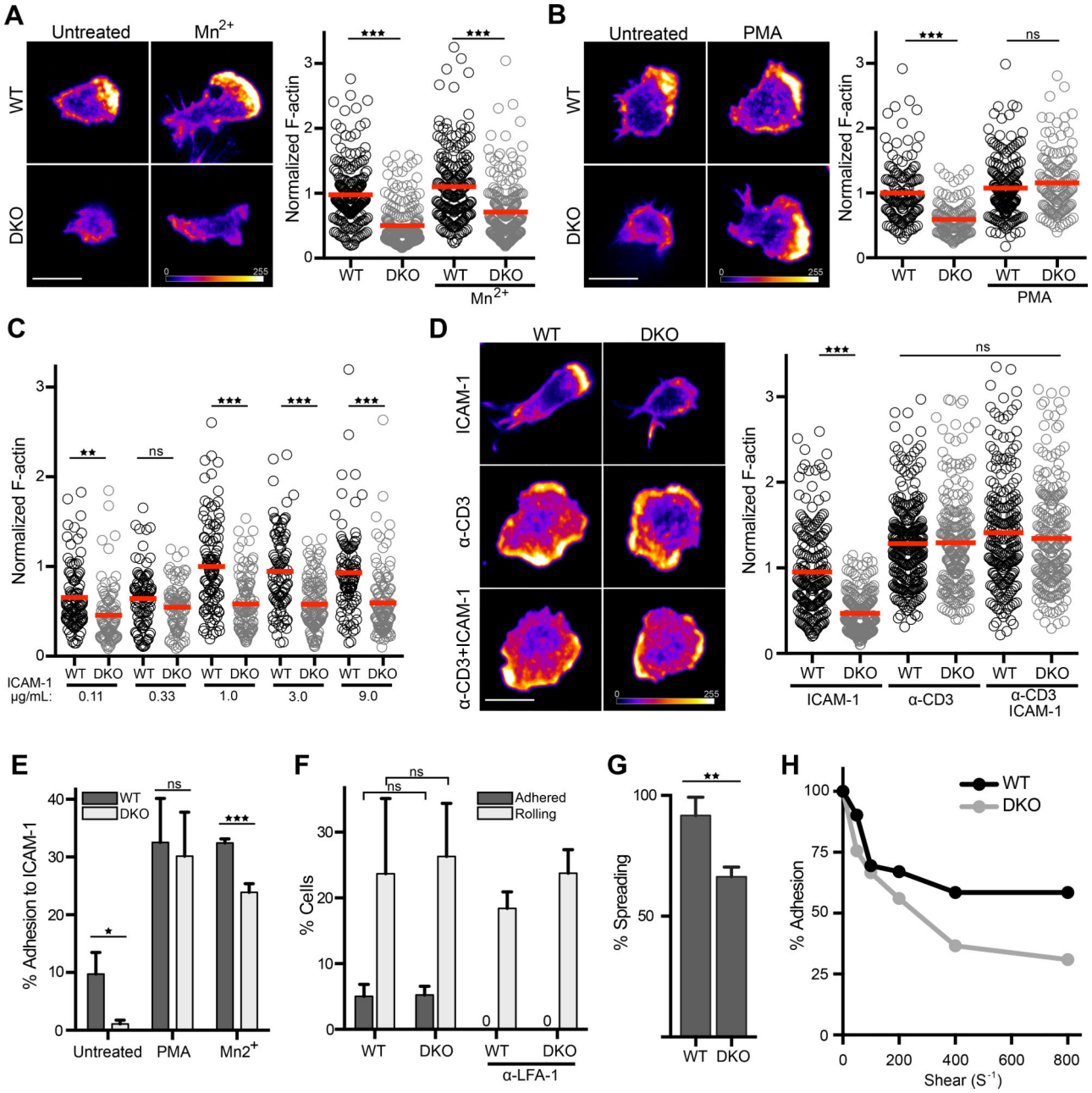

Figure 1. Crk proteins promote LFA-1 adhesion strengthening and actin reorganization

A and B) $CD4^+$ T cells were allowed to adhere for 20 mins to ICAM-1 coated coverslips in the presence or absence of (A) Mn^{2+} or (B) PMA, fixed, and stained with phalloidin. Right, quantification of phalloidin staining of individual cells, normalized to the WT untreated. Signal intensity is represented by a heat map. Scale bar, 10μm. Data pooled from 3 experiments. **C)** $CD4^+$ T cells were allowed to adhere to coverslips coated with increasing concentrations of ICAM-1, and phalloidin staining of individual cells was quantified and normalized to the 1ug/mL condition. **D)** $CD4^+$ T cells were allowed to adhere to surfaces for 20 mins that were coated with ICAM-1, anti-CD3, or both. Cells were fixed and stained with phalloidin. Right, quantification of phalloidin staining of individual cells, normalized to the

WT ICAM-1 condition. Scale bar, 10μm. Data were pooled from 2 experiments. **E)** $CD4^+$ T cell adhesion to ICAM-1 was measured using a standard plate-based adhesion assay. T cells were treated with PMA (to bypass inside-out signaling) or Mn^{2+} (to exogenously induce integrin conformational change). Data are mean +/− SD from 3 experiments. **F)** Percentage of T cells that rolled or adhered with $100s^{-1}$ shear rate on surfaces coated with ICAM-1, P-selectin, and SDF-1. Treatment with anti-LFA-1 antibody blocked all adhesion, showing that adhesion is dependent upon the LFA-1/ICAM-1 interaction. Data are mean +/− SD from 3 experiments. **G)** Percentage of adhered cells in (F) that subsequently spread. **H)** $CD4^+$ T cells were allowed to adhere in the absence of shear, and then the shear rate was increased every 2 min. For each shear rate, the percentage of remaining cells adhered was calculated. Data represent one experiment of 3. *p<0.05; **p<0.01; ***p<0.001; ns, not significant; by one-way ANOVA for comparison of multiple groups, or by a t-test for comparison of two groups.

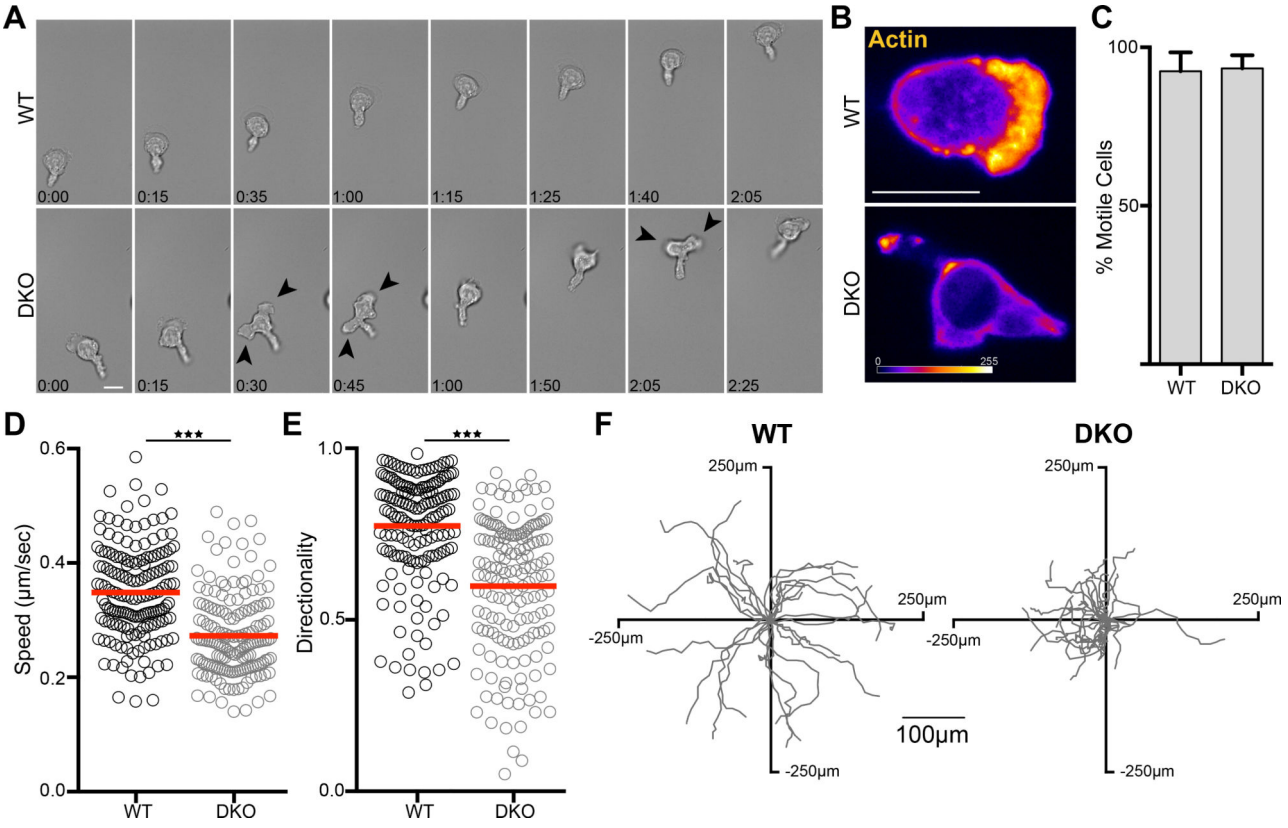

Figure 2. Crk proteins are required for leading edge formation and normal migration

A) $CD4^+$ T cells were allowed to adhere to ICAM-1 coated coverslips for 20 mins, washed, and time-lapse images were taken of migrating cells using DIC optics. Scale bar, 10μm. (see movies S1 and S2). Darts highlight multiple cell protrusions. **B)** $CD4^+$ T cells expressing Lifeact-GFP were treated as in (A) and time-lapse images were taken using confocal microscopy. Images are a projection of a 1μm total stack at the coverslip interface, with Lifeact-GFP intensity represented by a heat map. Scale bar, 10μm. (see Supplemental Movies 3 and 4). **C-F)** $CD4^+$ T cells were treated as in (A) and tracked over a 10 min period using DIC optics. **C)** Percentage of adhered T cells that were migratory. Data are mean +/− SD from 3 experiments. **D)** Average speed and **E)** Directionality of migrating T cells, calculated as net displacement divided by track length. Data were pooled from 4 experiments. **F)** Tracks from a single experiment of individual migrating T cells centered at the same starting point. *p<0.05; **p<0.01; ***p<0.001 by a t-test.

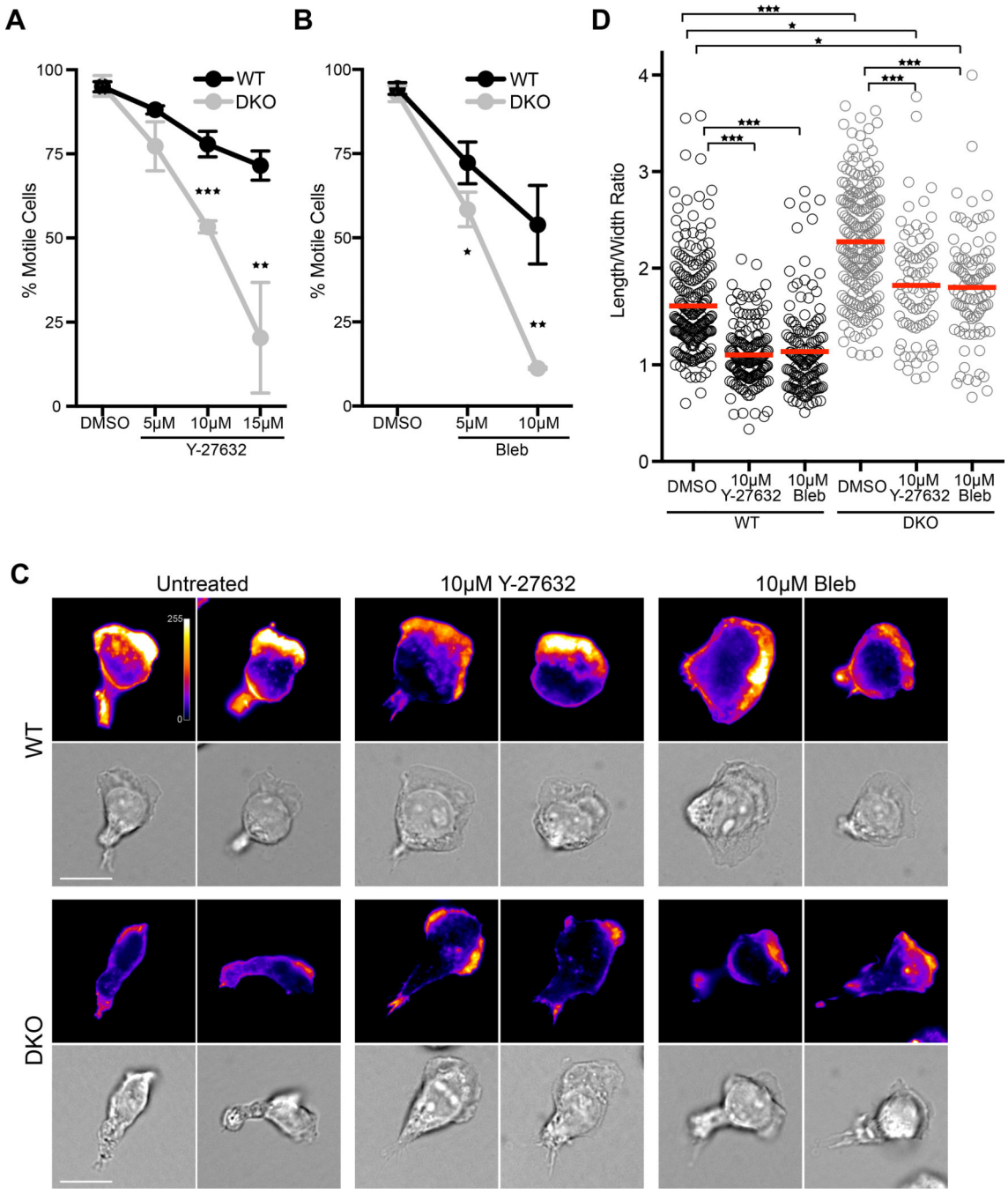

Figure 3. Migration of DKO T cells is more dependent on myosin activity

A and B) CD4$^+$ T cells were allowed to adhere to ICAM-1 coated coverslips for 20 mins, washed, and the percentage of migrating cells was calculated after 5 min pre-treatment with DMSO or with increasing concentrations of (A) Y-27632 or (B) S-nitro-blebbistatin. Data are mean +/− SD from 3 experiments. **C)** Representative images of migrating CD4$^+$ T cells treated with DMSO, 10μM Y-27632, or 10μM S-nitro-blebbistatin. Cells were fixed and stained with phalloidin. Scale bar, 10μm. **D)** Length/width ratios of individual cells migrating under the different treatments. Cells that were not migratory were predominantly

round and, thus, excluded from the analysis. Data are mean +/− SD from 3 experiments. *p<0.05; **p<0.01; ***p<0.001 by one-way ANOVA for comparison of multiple groups, or by a t-test for comparison of two groups.

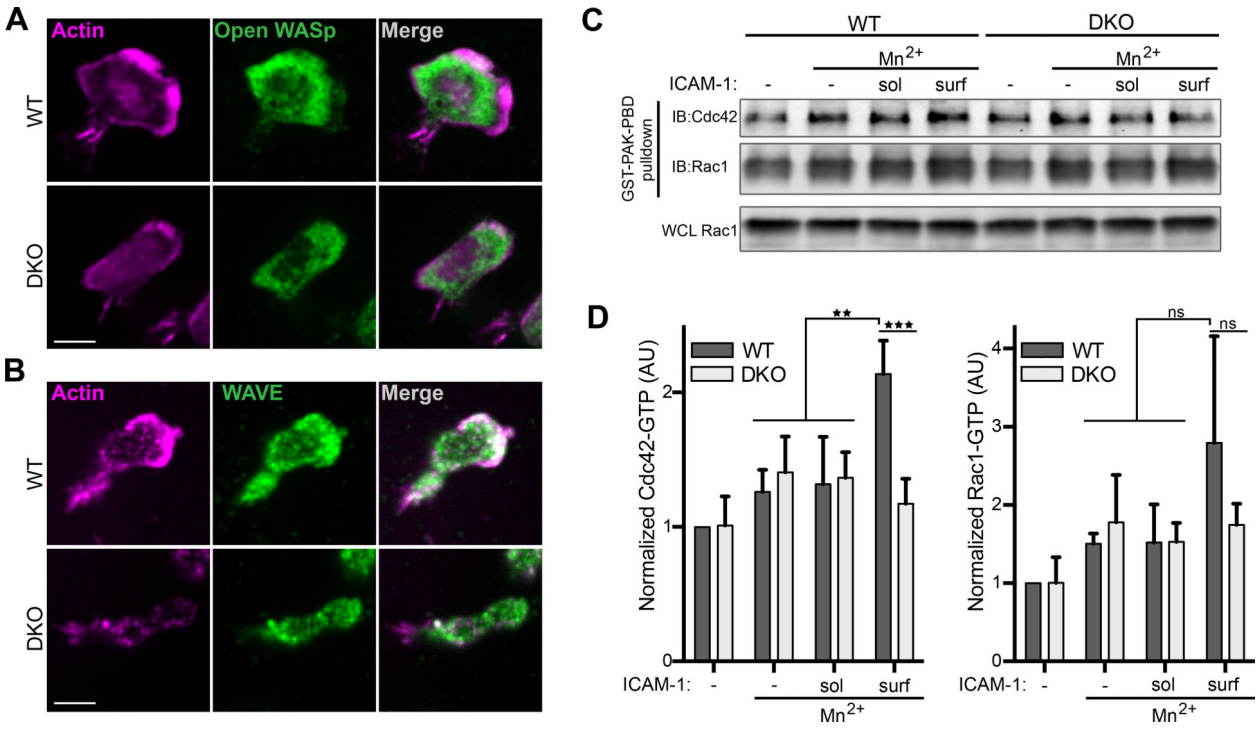

Figure 4. LFA-1 dependent Cdc42 activation is blunted in DKO T cells

A-B) $CD4^+$ T cells were allowed to migrate on ICAM-1 coated surfaces, fixed, and probed with fluorescent phalloidin to label F-actin and with an antibody that recognizes **A)** open WASp or **B)** total WAVE2. Scale bar, 10μm. **C and D)** $CD4^+$ T cells were treated with Mn^{2+} to activate LFA-1, followed by exposure to soluble or surface bound ICAM-1 for 20 min. Lysates were mixed with GST-PAK-PBD to pulldown GTP-bound GTPases. Representative western blot (C) and quantification of Cdc42-GTP (D, left) and Rac1-GTP (D, right). Data are mean +/− SD from 4 experiments. Densitometry was normalized to that of the WT untreated condition. *p<0.05; **p<0.01; ***p<0.001; ns, not significant; by one-way ANOVA.

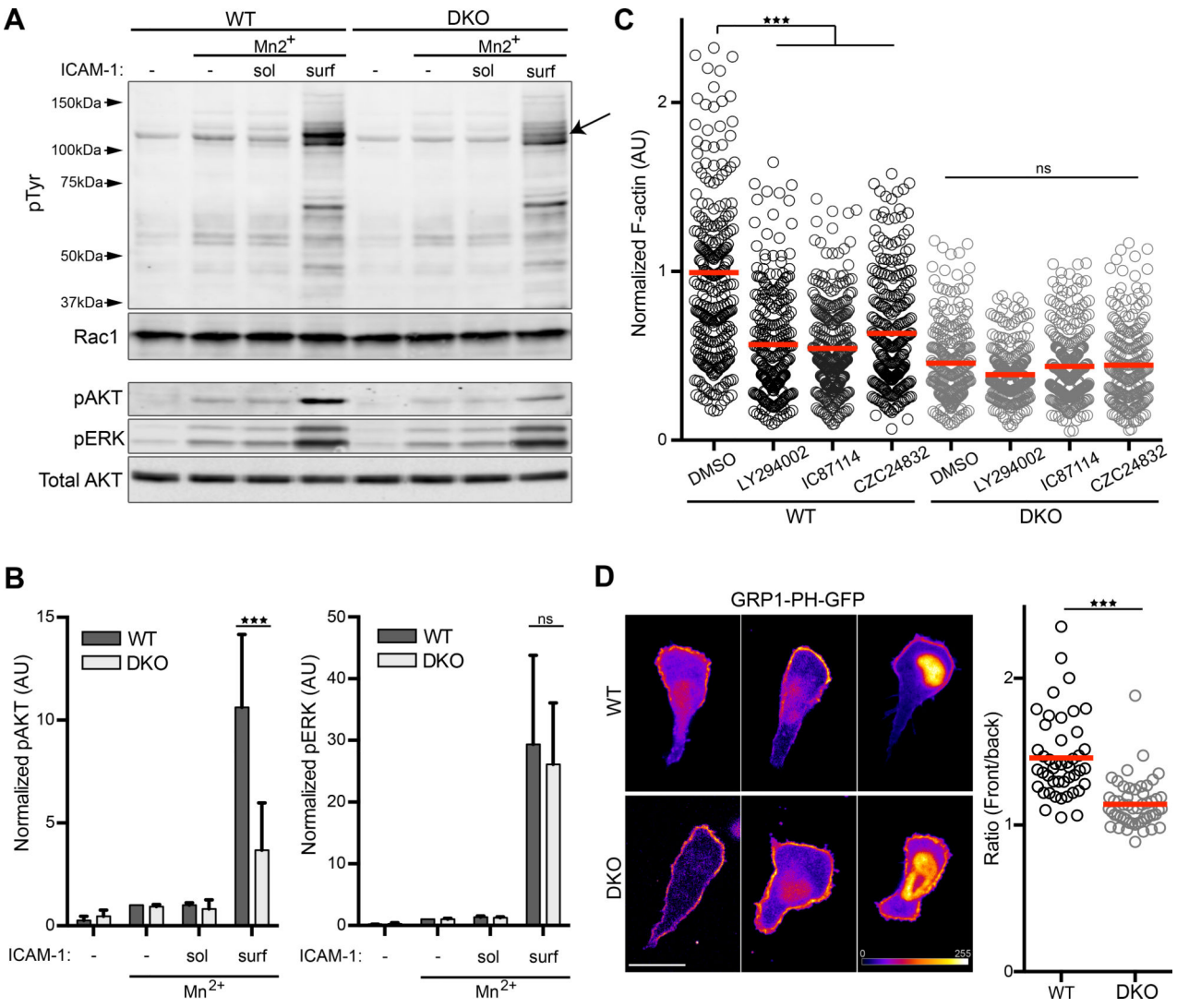

Figure 5. Crk proteins promote integrin mediated PI3K signaling

A) $CD4^+$ T cells were treated as in Fig. 4C, and lysates were immunoblotted with indicated antibodies. **(B)** Quantification of pAKT (left panel) and pERK (right panel). Values were normalized to the WT Mn^{2+} condition. Data represent mean +/− SD from 3 experiments. **C)** $CD4^+$ T cells were treated with Mn^{2+} and allowed to adhere to ICAM-1 coated surfaces in the presence or absence of the pan PI3K inhibitor LY-294002, or the specific inhibitors IC87114 (PI3Kδ) or CZC24832 (PI3Kγ). Cells were fixed, stained with fluorescent phalloidin, and total phalloidin staining per cell was quantified. Data were pooled from 3 experiments. **D)** $CD4^+$ T cells expressing the PIP_3 biosensor GRP1-PH-GFP were imaged while migrating on ICAM-1. GRP1-PH-GFP intensity is represented as a heat map. Right, Ratio of average GRP1-PH-GFP intensity at the leading edge vs the trailing edge on a cell-by-cell basis. Note that signal intensity for each cell was adjusted individually, to best reveal front-rear asymmetry Scale bar, 10μm. Data were pooled from 3 experiments. *p<0.05; **p<0.01; ***p<0.001; ns, not significant; by one-way ANOVA for comparison of multiple groups, or by a t-test for comparison of two groups.

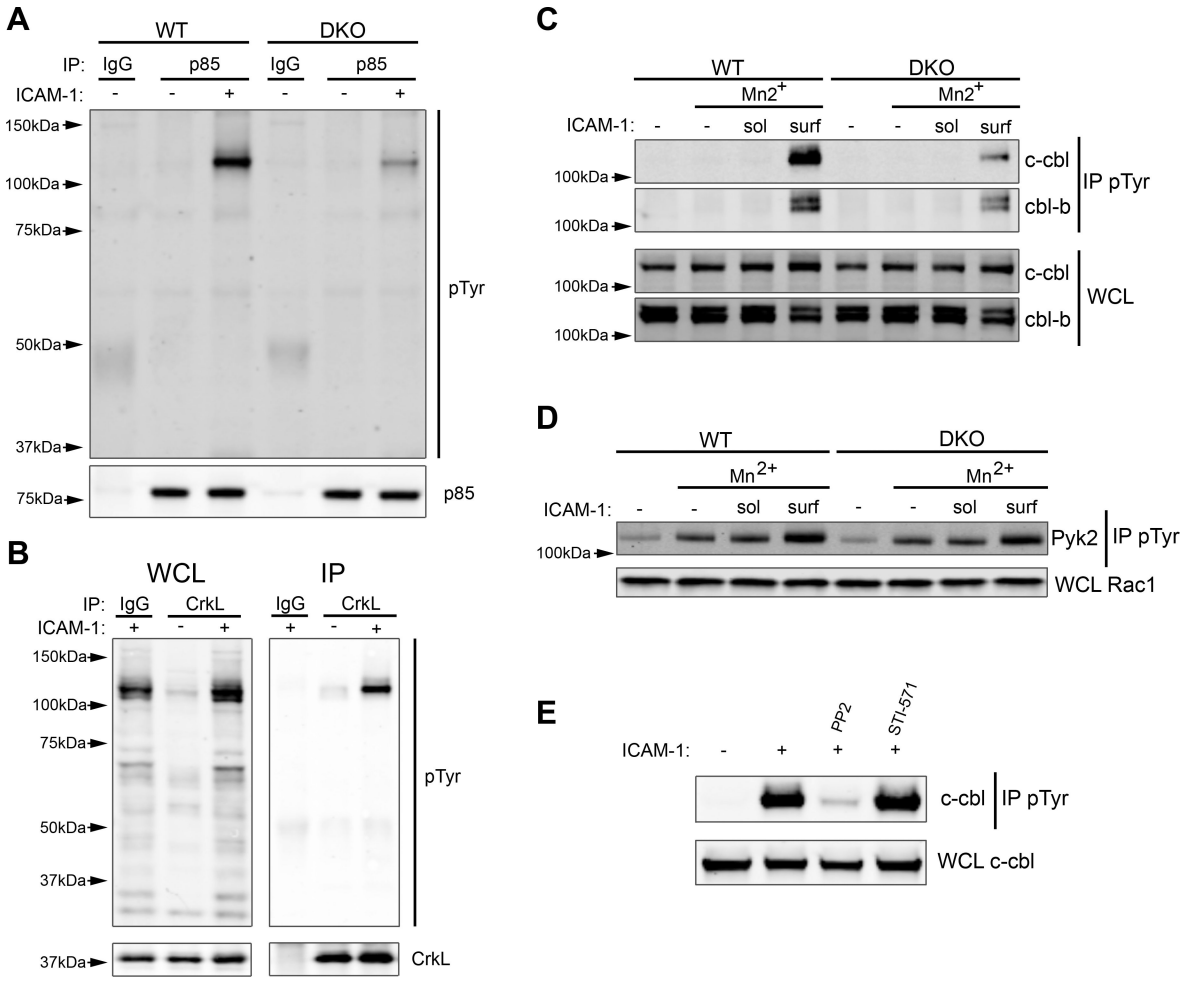

Figure 6. Crk proteins are necessary for phosphorylation of c-Cbl and its interaction with p85

A) $CD4^+$ T cells were treated with Mn^{2+} and then allowed to adhere to ICAM-1 coated plates for 20 min. Lysates were immunoprecipitated with anti-p85 and immunoblotted for pTyr. **B)** Cells were treated as in (A), except lysates were immunoprecipitated with anti-CrkL and immunoblotted for pTyr. **C)** $CD4^+$ T cells were treated with Mn^{2+} followed by exposure to soluble or surface bound ICAM-1 for 20 min. Lysates were immunoprecipitated with anti-pTyr and immunoblotted for c-Cbl and Cbl-b. **D)** Cells were treated as in (C), except lysates were immunoblotted for Pyk2. **E)** $CD4^+$ T cells were treated with Mn^{2+} and allowed to adhere to ICAM-1 coated plates in the presence of the indicated drugs for 20 min. Lysates were immunoprecipitated with anti-pTyr and immunoblotted for c-Cbl. Immunoblots are representative of 3–5 experiments.

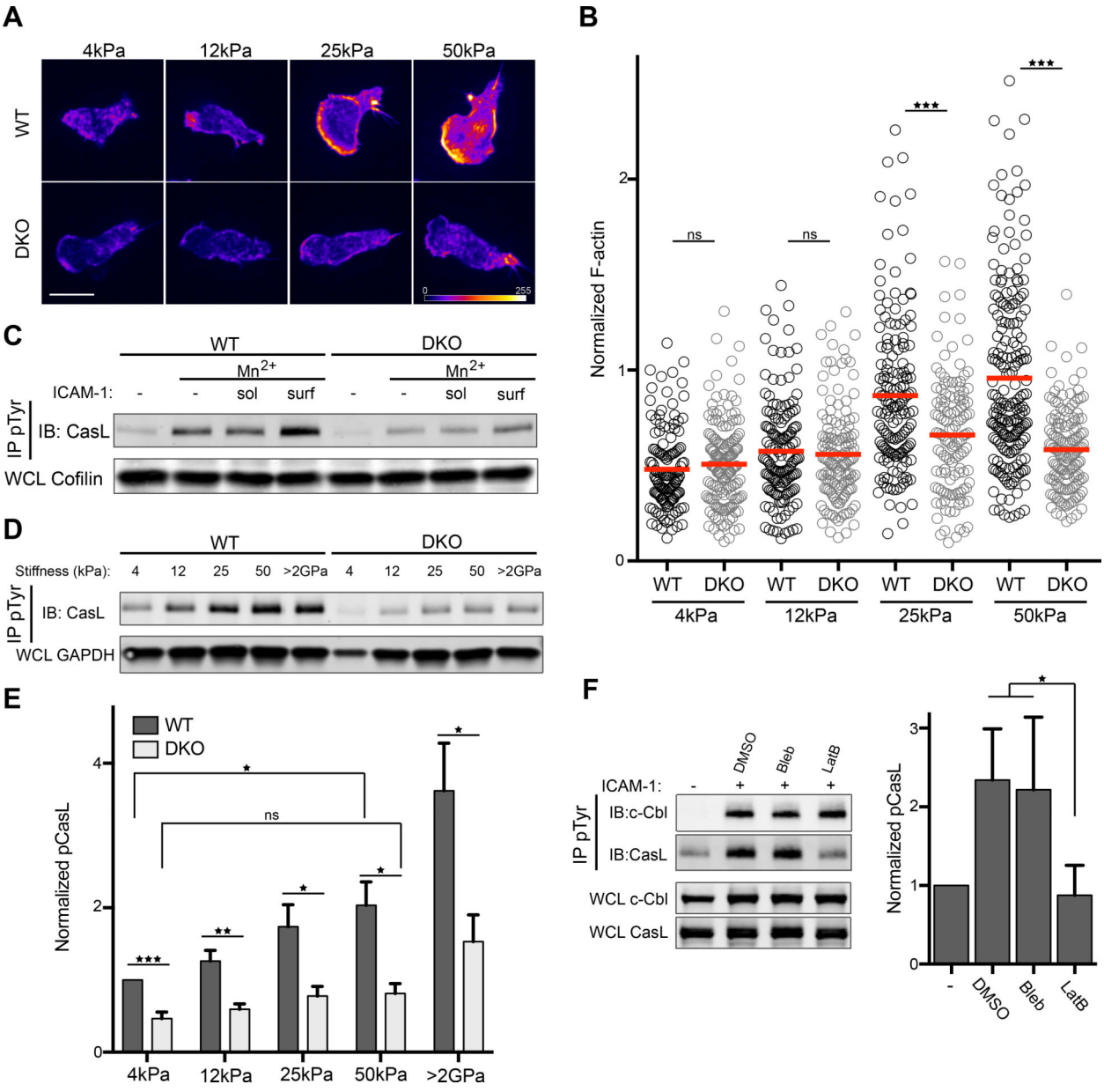

Figure 7. LFA-1 dependent mechanosensing requires Crk proteins

A-B) CD4$^+$ T cells were treated with Mn^{2+} and allowed to adhere to ICAM-1 coated hydrogels of increasing stiffness. Cells were fixed, stained with fluorescent phalloidin and imaged. Phalloidin intensity is represented as a heat map. Scale bar, 10μm. **B)** Quantification of total phalloidin staining per cell. Values were normalized to WT, 50kPa condition. Data is pooled from 2 experiments. **C)** CD4$^+$ T cells were treated with Mn^{2+}, followed by exposure to soluble or surface bound ICAM-1 for 20 mins, lysed and immunoprecipitated with anti-pTyr, followed by immunoblot for CasL. **D)** CD4$^+$ T cells were treated with Mn^{2+} and allowed to adhere to ICAM-1 coated hydrogels of increasing stiffness, lysed, immunoprecipitated with anti-pTyr, and immunoblotted for CasL. **E)** Quantification of pCasL abundance in cells plated on hydrogels of different stiffnesses. Data are mean +/− SD

from 3 experiments. **F)** $CD4^+$ T cells were treated with Mn^{2+} and allowed to adhere to ICAM-1 coated surfaces for 10 min, followed by treatment with the indicated drugs for an additional 10 min. Cells were lysed, immunoprecipitated with anti-pTyr, and immunoblotted for CasL and c-Cbl. Right, quantification of pCasL abundance. Data are mean +/− SD from 3 experiments. *p<0.05; **p<0.01; ***p<0.001; ns, not significant; by one-way ANOVA.

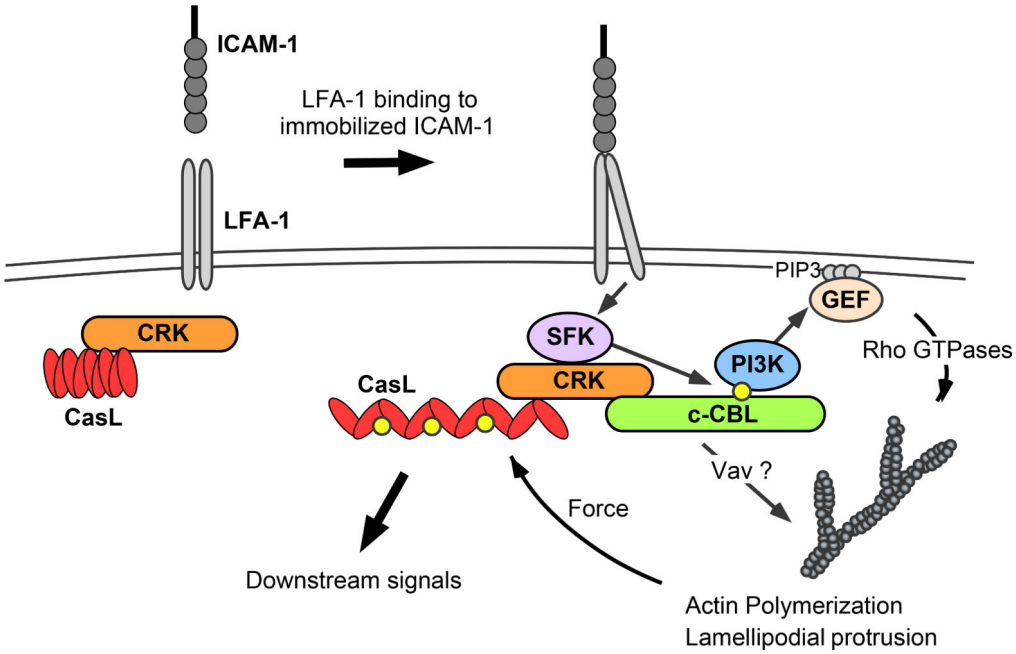

Figure 8. Proposed model for Crk-dependent integrin signaling

Our data suggest a model in which engagement of LFA-1 by immobilized ligands activates Src family kinases (SFK) and induces the binding of preformed Crk/CasL complexes to c-Cbl. Formation of this complex promotes SFK-dependent phosphorylation of c-Cbl (yellow dots), which in turn creates a binding site for the p85 subunit of PI3K. This activates PI3K catalytic function, resulting in localized production of PIP_3. Recruitment of guanine exchange factors (GEF) to PIP_3-rich membrane regions, and possibly also to the Crk/c-Cbl complex itself, then induces Rho GTPase activation, resulting in actin polymerization and leading-edge formation. Actin polymerization also provides the force necessary to open the CasL substrate domain and enable its phosphorylation (most likely also by SFKs). Phospho-CasL then serves as a scaffold for additional signaling molecules that direct cellular responses to the perceived mechanical cues.